2023年2月 February，2023

矿 床 地 质
MINERAL DEPOSITS

第42卷 第1期
42（1）：128~156

文章编号：0258-7106（2023）01-0128-29　Doi: 10. 16111/j. 0258-7106. 2023. 01. 009

斑岩铜-钼-金矿床：构造环境、成矿作用与控制因素*

杨　航[1]，秦克章[2,3]，吴　鹏[1**]，王　峰[1,4]，陈福川[1]

（1 昆明理工大学 国土资源工程学院，有色金属矿产地质调查中心 西南地质调查所，云南 昆明　650093；2 中国科学院矿产资源研究重点实验室 中国科学院地质与地球物理研究所，北京　100029；3 中国科学院大学，北京　100049；4 云南冶金资源股份有限公司，云南 昆明　651100）

摘　要　斑岩型矿床作为全球 Cu、Mo、Au、Re 等战略性矿产的主要来源，是国际矿床学界和矿业界长期关注的热点。最新研究表明，斑岩矿床既可以产于俯冲带岩浆弧环境，也可以产于与俯冲无关的非弧环境（主要包括碰撞造山环境、陆内造山环境以及活化克拉通边缘及内部），后者发育于中国大陆。文章在总结全球斑岩矿床时空分布规律的基础上，重点从成矿斑岩成因与成矿动力学机制、成矿金属来源、蚀变-矿化分带等方面，综述了 2 类斑岩矿床的研究进展，阐释并总结了控制斑岩成矿的主要因素与机制，以及相关研究方法。研究表明，全球斑岩矿床集中产于 3 大成矿域，形成时代以中、新生代为主。其中，环太平洋成矿域斑岩矿床时空分布不均，集中发育于美洲西海岸，主要形成于白垩纪以来较年轻的几个短暂时期；古亚洲洋成矿域斑岩矿床形成时间跨度于奥陶纪—早白垩世，具有“西 Cu-Au 东 Cu-Mo、早 Cu-Au 晚 Cu-Mo”的成矿特征；特提斯成矿域主要发育三叠纪以来的斑岩矿床，主体沿造山带分布，时间分布不均，同一构造带内发育不同时期的斑岩成矿作用；中国斑岩矿床与 3 大成矿域既显示出对应性，也有独特性和复杂性。弧环境成矿岩浆、金属 Cu(Au)主要来源于交代地幔楔，大洋岩石圈板块俯冲是其根本性动力学机制；而非弧环境成矿岩浆、金属 Cu(Au)主要来自镁铁质新生/拆沉下地壳或富集地幔，大陆碰撞和陆内俯冲是其主要诱发机制。碰撞造山环境斑岩矿床矿化主要发生在叠加于钾硅酸盐化之上的绢英岩化阶段有别于弧斑岩矿床。两类斑岩均具有高氧逸度、富水和挥发分等特征，岩浆源区、岩浆性质、岩浆混合作用等可能是大型斑岩矿床的控制因素。岩浆岩 Hf-Nd 同位素、锆石和磷灰石等岩浆副矿物、镁铁质包体等，为约束斑岩成矿岩浆条件及其演变过程提供了思路。

关键词　地质学；斑岩矿床；时空分布；构造环境；成矿作用；控制因素

中图分类号：P618.41；P618.51；P618.65　**文献标志码**：A

Tectonic setting, mineralization and ore-controlling factors of porphyry Cu-Mo-Au deposits

YANG Hang[1], QIN KeZhang[2,3], WU Peng[1], WANG Feng[1,4] and CHEN FuChuan[1]

(1 Faculty of Land Resource Engineering/Southwest of Geological Survey, Geological Survey Center for Non-ferrous Mineral Resources, Kunming University of Science and Technology, Kunming 650093, Yunnan, China; 2 Key Laboratory of Mineral Resources, Institute of Geology and Geophysics, Chinese Academy of Sciences, Beijing 100029, China; 3 University of Chinese Academy of Sciences, Beijing 100049, China; 4 Yunnan Metallurgy Resources Exploration Co., Ltd., Kunming 651100, Yunnan, China)

Abstract

Porphyry deposits, globally the main sources of strategic minerals such as Cu, Mo, Au and Re, have always been the hot topics for international mineral deposit researchers and mining indreustry. The latest research indi-

---

* 本文得到国家自然科学基金项目（编号：41102049）、云南省“万人计划”青年拔尖人才专项（编号：YNWR-QNBJ-2018-272）、云南省矿产资源预测评价工程实验室（2010）和云南省地质过程与矿产资源创新团队（2012）联合资助

第一作者简介　杨　航，男，1994 年生，博士研究生，矿产普查与勘探专业。Email: 983719232@qq.com

* * 通讯作者　吴　鹏，男，1981 年生，教授，主要从事矿产普查与勘探的教学与科研。Email: 76902594@qq.com

收稿日期　2022-06-20；改回日期　2023-01-06。孟秋熠编辑。

cates that porphyry deposits formed in either the magmatic arc setting of subduction zone or non-arc setting unrelated to subduction (mainly includes collisional orogenic setting, intracontinental orogenic setting, and in the edge and interior of re-activated craton), and the latter is widely formed in Chinese mainland. By summarizing the spatio-temporal distribution of global porphyry deposits, this paper focuse on discussing the research progress of two types of porphyry deposits from the aspects of petrogenesis and metallogenic dynamic mechanism, source of ore-forming metals, alteration-mineralization zoning, and then discusses and summarizes the main ore-controlling factors and mechanisms controlling porphyry mineralization, as well as related research methods. The research shows that porphyry deposits are concentrated in the three major tectonic, and are mainly formed in the Mesozoic and Cenozoic. Among them, porphyry deposits in the Circum Pacific metallogenic domain are distributed unevenly in time and space, mainly developed in the West Continental margin of America, and mainly formed in several short periods since the Cretaceous; The porphyry deposits in the Paleo-Asian Ocean metallogenic domain are formed in the Ordovician to early Cretaceous, and show the metallogenic characteristics of "Western Cu-Au, eastern Cu-Mo, early Cu-Au and late Cu-Mo"; In the Tethys metallogenic domain, porphyry deposits are mainly formed since the Triassic, they are distributed along the orogenic belts, but the temporal distribution is uneven, and the porphyry mineralization formed in different periods in the same tectonic belt; At the same time, the porphyry deposits in China have correspondency, uniqueness and complexity with the three metallogenic domains. The ore-forming magmas and Cu(Au) metals in arc setting are mainly derived from metasomatic mantle wedge, and the subduction of oceanic lithosphere plate is the fundamental dynamic mechanism. In contrast, the ore-forming magmas and Cu(Au) in non-arc setting are mainly derived from the mafic juvenile/delaminated lower crust or enriched mantle, and continental collision and intracontinental subduction are the main inducing mechanisms. The mineralization of porphyry deposits in collisional orogenic setting mainly forms in phyllic alteration stage superimposed on the K-silicatie zones, which is different from arc porphyry deposits. The two types of ore-forming magmas are characterized by high oxygen fugacity, rich water content and volatile components. We suggest that magma source, magma properties and magma mixing may be the ore-controlling factors of large porphyry deposits. Hf-Nd isotope of magmatic rocks, magmatic accessory minerals such as zircon and apatite, and mafic enclaves may provide ideas to constrain the magmatic conditions and evolution process of porphyry mineralization.

Key words: geology, porphyry deposit, spatio-temporal distribution, tectonic setting, mineralization, ore-controlling factors

斑岩型矿床是产于中酸性浅成-超浅成侵入岩中及其内外接触带附近,以浸染状-细脉浸染状为主要矿化样式的一类岩浆热液矿床,具有埋藏浅、品位低、规模大等特点,为全球提供了75%的Cu、50%的Mo、20%的Au,以及绝大部分的Ag、Zn、Sn、W、Re等,是最具有经济意义的矿床类型之一(Cooke et al.,2005;Richards,2009;Sillitoe,2010)。根据有用金属元素的含量可将斑岩矿床分为斑岩型Au、Cu、Mo、W及Sn矿床以及它们之间的过渡类型。如许多斑岩型Cu矿床中常含有Au/Mo的富集,形成斑岩型Cu-Au或斑岩型Cu-Mo或介于二者的斑岩型Cu-Au-Mo矿床(Singer et al.,2008)。中国主要发育斑岩型Cu矿床和斑岩型Mo矿床,其中斑岩型Cu矿床是中国最主要的Cu矿床类型。最新资料显示,中国斑岩Cu矿总资源量约为47 Mt,占全国Cu资源储量的42%(Yang et al.,2019)。由于斑岩型矿床的经济价值巨大,百余年来全球的勘探学家和矿床学家开展了大量的勘探和研究工作,取得了丰硕的研究成果,无论是在找矿效果和成矿理论方面都取得了重要进展,并逐渐形成较为完整的理论与学科体系。

经典的斑岩成矿理论是基于俯冲带岩浆弧环境斑岩矿床建立起来的(Lowell et al.,1970;Sillitoe,1972;1997)。近年来研究发现,斑岩矿床还可以产于与俯冲无关的非弧环境,该类矿床广泛发育于中国大陆。本文主要从时空分布规律、产出构造环境、成矿斑岩成因与成矿动力学机制、成矿金属来源、蚀变-矿化分带等方面,系统总结了两类斑岩型矿床(岩浆弧斑岩矿床和非弧斑岩矿床)的研究进展,阐

释了岩浆源区、岩浆性质(氧逸度、含水量、挥发分等)以及岩浆混合作用等控制斑岩成矿的因素和机制,及其主要研究内容和方法,旨在增进对斑岩Cu-Mo-Au矿床的认识和理解。

1　全球斑岩矿床的时空分布规律

全球的斑岩型矿床集中产于环太平洋、古亚洲洋和特提斯三大成矿域内(图1),形成时代以中、新生代为主(约占94.5%),另有少量产于前寒武纪造山带(芮宗瑶等,2004)。

1.1　环太平洋成矿域

尽管古太平洋板块俯冲开始的时间尚存争议,但已有的观点表明其最早可能起始于侏罗纪甚至更早(Zhou et al., 2006; Wang et al., 2011; Seton et al., 2012; Zhu et al., 2019),并且经历了多个板块的多次漂移/俯冲方向的转变(Sharp et al., 2006; Sun et al., 2007; 2020),形成了现存规模最为宏大、体系最为完整的斑岩成矿域,由东、西2条俯冲带组成,经典斑岩Cu成矿理论即起源于此(Lowell et al., 1970)。东、西2条俯冲带内斑岩矿床的时空分布很不均匀,主要成矿金属类型也有差异(图1)。

空间上,环太平洋成矿域的斑岩矿床主要分布在东太平洋俯冲带,且全球最大的超大型斑岩Cu矿床中的80%(20个)都分布在这条细长的成矿带上。其中,仅南美智利就集中了全球40%以上的斑岩Cu矿,拥有El Teniente、Chuquicamata和Rio Blanco-Los Bronces等10个储量排名全球前25的超大型斑岩Cu矿床(Cooke et al., 2005)。除Cu以外,这些矿床通常还发育Mo、Au资源,如El Teniente和Chuquicamata矿床Mo的金属量均在1.8 Mt以上,Au的金属量也在300 t以上(Cooke et al., 2005)。与此形成鲜明对比的是,西太平洋俯冲带斑岩矿床无论从数量还是从单个矿床的储量上都要少且小很多,矿床主要金属类型也比较单一,几乎没有含Mo的斑岩矿床(Cooke et al., 2005; Sun et al., 2010)。带内大—中型

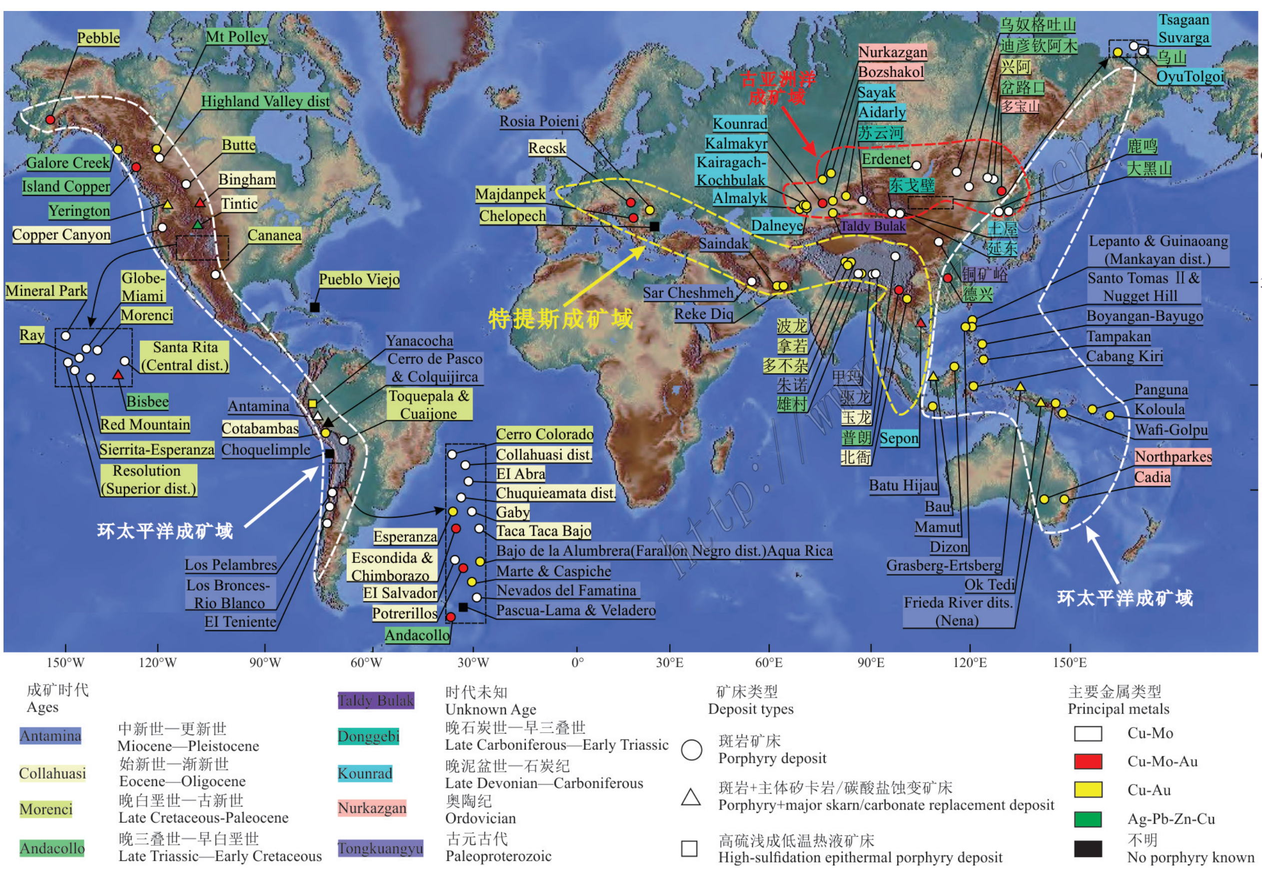

图1　全球大型斑岩矿床的分布和三大成矿域(据Sillitoe, 2010; Yang et al., 2019; Wang et al., 2020修改)

Fig. 1　Distribution of large-scale porphyry deposits in the world and three major metallogenic domains (modified from Sillitoe, 2010; Yang et al., 2019; Wang et al., 2020)

斑岩Cu-Au矿床主要分布在中国东部的德兴和长江中下游地区以及菲律宾岛到东帝汶之间。其中，菲律宾岛到东帝汶之间的Cu-Au矿床中Au含量较高，但不含Mo，被认为是西南太平洋年轻的弧后盆地闭合的产物（Braxton et al.，2012）。而中国东部的德兴和长江中下游斑岩Cu-Au矿床产出的构造环境和形成的动力学背景存在古太平洋俯冲和华南陆内造山（再造）之争（Ling et al.，2009；Sun et al.，2012；Wang et al.，2013；Zhang et al.，2017）。

时间上，环太平洋的斑岩矿床主要形成于几个较年轻的短暂时期（图1）。其中，南美洲的斑岩矿床主要形成于始新世—渐新世和中新世—更新世2个时期；北美洲除了Bingham形成于始新世以外，其他大型—超大型矿床主要形成于晚三叠世—早白垩世和晚白垩世—古新世2个时期；西南太平洋斑岩Cu-Au矿床主要形成于中新世—更新世，而东亚陆缘主要是侏罗纪、白垩纪的斑岩Cu-Au矿床。

深入的研究指出，环太平洋成矿域内许多大型、超大型斑岩Cu-Au矿床在空间上与正在俯冲的洋中脊有对应关系（Cooke et al.，2005；Sun et al.，2010）。因此，认为造成环太平洋成矿域斑岩Cu-Au矿床分布不均的原因，可能与东太平洋俯冲带数量较多、规模较大的洋脊俯冲有关（Sun et al.，2010）。因为该过程中，热的、年轻的洋壳容易发生部分熔融形成富集Cu、Au的埃达克岩，有利于斑岩Cu、Au矿的形成（Peacock et al.，1994；Sun et al.，2010；2013）。而造成金属Mo存在差异的原因，可能与东太平洋白垩纪富Mo沉积物比西太平洋更发育和东、西太平洋俯冲体制差异有关。白垩纪大洋缺氧事件所形成的富Mo黑色页岩和弧前富Mo陆源沉积物为东太平洋陆缘俯冲带俯冲板片部分熔融形成富Mo原始岩浆提供了主要Mo源（孙卫东等，2015）。

1.2　古亚洲洋成矿域

古亚洲洋闭合形成的中亚造山带的古亚洲洋成矿域是三大成矿域中最老的。该成矿域经历了新元古代到晚石炭世大洋板块俯冲体系，以及后续的碰撞、闭合及地体拼贴等重要过程，形成了全球最大的增生型造山带（Windley et al.，2007；Xiao et al.，2010；Yuan et al.，2010；Cai et al.，2011）。域内既发育有增生造山阶段的弧环境相关矿床（蛇绿岩型、斑岩型、VMS），也发育与碰撞造山（造山型）和后碰撞陆内岩石圈伸展相关的大陆环境矿床（岩浆型、斑岩型、热液型、砂岩型等）（Qin et al.，2011；秦克章等，2017；Sun et al.，2020）。其中，斑岩型是古亚洲洋成矿域Cu-Au矿床最为重要的成矿类型，发育蒙古国的Oyu Tolgoi（Wainwright et al.，2011）、乌兹别克斯坦的Kal'makyr（Zhao et al.，2017）和哈萨克斯坦的Aktogay-Aiderly（Li et al.，2018）3个储量排名全球前25的超大型斑岩Cu-Au矿床，以及土屋-延东、多宝山等大型-超大型斑岩Cu矿（Xiao et al.，2017；Zhao et al.，2018）。域内重要斑岩型Cu-Au矿床及相关浅成低温热液和矽卡岩型Au-Cu矿床主要分布巴尔喀什湖南北、Kurama山脉和蒙古国南。这些斑岩矿床形成时间跨度较大，主体形成于晚泥盆世—石炭纪和晚三叠世—早白垩世，也有部分矿床形成于奥陶纪，具有“西Cu-Au东Cu-Mo、早Cu-Au晚Cu-Mo”的成矿作用特征（高俊等，2019）。如成矿域西部发育古生代（晚泥盆世—石炭纪）的Kal'makyr、Aiderly等Cu-Au矿床，而东部主要为中生代（晚三叠世—早白垩世）的乌奴格吐山、Tsagaan Suvarga等Cu-Au矿床（图1）。

古亚洲洋洋壳俯冲增生、陆-陆碰撞和后碰撞伸展等不同时期地质环境中，虽然均有斑岩Cu-Au成矿作用发生，但域内大型-超大型斑岩Cu-Au矿床主要形成于古亚洲洋俯冲形成的不同时期增生岛弧环境，大规模斑岩Cu-Au成矿出现在洋盆演化末期、或即将关闭时的成熟岛弧环境（Wainwright et al.，2011；薛春纪等，2016；Xiao et al.，2017；Gao et al.，2018）。而中生代斑岩Mo矿集中爆发成矿则分别受控于古亚洲洋体系后碰撞、古太平洋体系同俯冲及古太平洋体系俯冲回撤诱发的岩石圈减薄事件等不同大地构造背景（Chen et al.，2017；高俊等，2019）。

1.3　特提斯成矿域

横亘于地球中纬度地区的特提斯碰撞造山带，是全球规模最宏大、最年轻的陆-陆碰撞造山带。它由一系列微陆块或地体拼贴而成，经历了复杂的俯冲、增生和碰撞造山过程，形成了全球大陆地质现象最丰富、特提斯洋发育最典型、矿产和油气资源最丰富的地域（任纪舜等，2006；邓军等，2010；Hou et al.，2015a；Ding et al.，2017；吴福元等，2020；Zhu et al.，2022）。该带经历了古生代—新生代不同时期原-古-新特提斯洋的洋-陆俯冲和随后的陆-陆碰撞过程，因此既发育俯冲阶段的成矿作用，又发育碰撞和后碰撞阶段的成矿作用，并且以斑岩成矿作用为主导，带内古-新特提斯洋演化和斑岩成矿作用包括以下5个过程：

（1）古特提斯洋俯冲成矿：成矿作用主要集中在青藏高原东南缘三江地区。晚三叠世，甘孜—古特提斯洋西向俯冲于中咱地块之下，于义敦岛弧带发育大规模的增生造山相关岩浆活动，伴生了一套与古特提斯洋俯冲岩浆活动相关的Cu-Mo-Ag-Pb-Zn-Hg成矿系统（Chen et al., 2017; Yang et al., 2017）。南北段板块俯冲的角度不同造就了不同的成矿环境，相应地形成了不同的岩石组合和矿床类型（杨立强等，2015）。北段昌台弧，俯冲角度较陡，发育呷村特大型VMS Ag-Pb-Zn多金属矿床（~217 Ma，Hou et al.，2003a），并伴有Cu-Mo-Au矿化；南段中甸弧，俯冲角度较缓，发育晚三叠世普朗—松诺—欠虽带和春都—雪鸡坪—烂泥塘带斑岩矿床，成矿时代主要集中于219~215 Ma（图1）（李文昌等，2010；Chen et al.，2014；Wang et al.，2021）。

（2）古特提斯洋碰撞成矿：包括同碰撞和后碰撞阶段，成矿作用主要集中于班公湖-怒江缝合带。该缝合带南北两侧分别发育以昂龙岗日-班戈岩浆弧和扎普-多不杂岩浆弧（包括多不杂火山岩浆弧、日土-材玛-弗野岩浆弧）为代表的成岩-成矿作用。前者主要形成一些矽卡岩型矿点（如插虚果棚矽卡岩型Cu-Fe矿床、桑日矽卡岩型Au-Cu矿床、班戈县青龙乡矽卡岩型Pb-Zn矿点、拉青Cu矿点等，耿全如等，2011）；后者分别形成了以多龙矿集区为代表的斑岩型Cu-Au多金属矿床（包括多不杂、波龙、地堡那木岗、拿若、荣那等）（120~110 Ma，图1，曲晓明等，2006a；2006b；Li et al.，2014；Wei et al.，2017）和以弗野富磁铁矿和材玛铁锰多金属矿为代表的Fe多金属矿床（成矿岩体年龄，弗野：130 Ma，材玛：164 Ma，耿全如等，2011）。

（3）新特提斯洋俯冲成矿：成矿作用时空分布不均，主要集中于冈底斯、巴基斯坦以及东南欧一带。其中，越来越多的证据表明新特提斯洋在晚三叠世就开始了向北俯冲（Wang et al.，2016；Zhu et al.，2022）。因此，位于青藏高原南部冈底斯中段岩浆弧的雄村斑岩Cu-Au矿集区（172~161 Ma，Lang et al.，2014；Tafti et al.，2014）和则莫多拉矽卡岩型Cu-Au矿床（~151 Ma，Wang et al.，2017）属于新特提斯俯冲成矿作用的产物；而新特提斯洋在巴基斯坦闭合时间较晚，中新世俯冲形成的Chagai陆缘弧呈东西向展布，宽190 km，长约400 km，带内岩浆岩发育，并赋存有Saindak和Reko Diq大型-超大型斑岩Cu-Au矿床和一系列中小型斑岩Cu-Au矿（图1），成矿时代主要集中于24~10 Ma（Perelló et al.，2008）；欧洲东南部，新特提斯俯冲产生一套晚白垩世的钙碱性弧岩浆，发育Majdanpek、Bor、Elatsite、Moldova Noua等一系列的斑岩型Cu-Au矿床和高硫型浅成低温热液矿床，构成Bananitic成矿带（BMMB；Ciobanu et al.，2002），这些矿床主要形成于92~84 Ma（Singer et al.，2005；2008）。

（4）新特提斯洋碰撞成矿：随着新特提斯洋的闭合，印度和欧亚大陆开始进入全面碰撞阶段，随后发育一系列与碰撞相关的岩浆活动和成矿作用，且遍布整个特提斯造山带，以青藏高原碰撞造山带成矿作用最为典型。在青藏高原，印度-欧亚大陆在65 Ma发生初始碰撞（莫宣学等，2003；侯增谦等，2006a；2006b），碰撞阶段代表性矿床为沿青藏高原南部冈底斯带北缘分布的亚圭拉斑岩-矽卡岩型Pb-Zn-Ag矿（65 Ma，Zhao et al.，2015）和沙让斑岩型Mo矿（52.3 Ma，秦克章等，2008；Zhao et al.，2014）。冈底斯带内还发育白垩纪花岗岩岩基、同碰撞冈底斯岩基和林子宗火山岩（莫宣学等，2003；Zhu et al.，2017；2019）。

（5）新特提斯洋碰撞后成矿：碰撞后成矿指印度-欧亚大陆主碰撞后的成矿作用（也称后碰撞成矿）。后碰撞斑岩矿床贯穿特提斯成矿域的绝大部分地区，由北西向南东，依次由伊朗Kerman斑岩Cu成矿带、冈底斯中新世斑岩Cu-Mo成矿带、缅甸斑岩Cu-Mo成矿带和三江斑岩Cu-Au成矿带等几条较大的斑岩成矿带构成（图2），其中① 伊朗Kerman斑岩Cu成矿带呈北西—南东向展布，绵延近1500 km，发育大量新生代岩浆岩，赋存有Sar Cheshmeh（储量排名全球前25的超大型斑岩Cu-Au矿床之一，~12.2 Ma，张洪瑞等，2013）和Sungun两个大型和一系列中小型斑岩矿床。这些矿床由北西到南东，成矿年龄逐渐变小，但主体集中于24~10 Ma（Hou et al.，2015a）；② 冈底斯中新世斑岩Cu-Mo成矿带是后碰撞斑岩矿床中最为瞩目的，目前已经探明的Cu金属量超过了25 Mt，包括了驱龙、甲玛等超大型斑岩Cu-Mo矿床和朱诺、冲江、岗讲等一系列大中小型斑岩矿床，这些矿床的形成时代集中于24~15 Ma（Hou et al.，2004；Yang et al.，2009；Leng et al.，2013；Li et al.，2017；Sun et al.，2018）；③ 缅甸斑岩成矿带呈南北向展布，主要包括西缅甸始新世的斑岩型Cu-Au矿床（如Shangalon-Kyungalon矿）和滇缅马苏西部地块的Sn-W矿床（如Mawchi矿），它们的成岩成矿作用

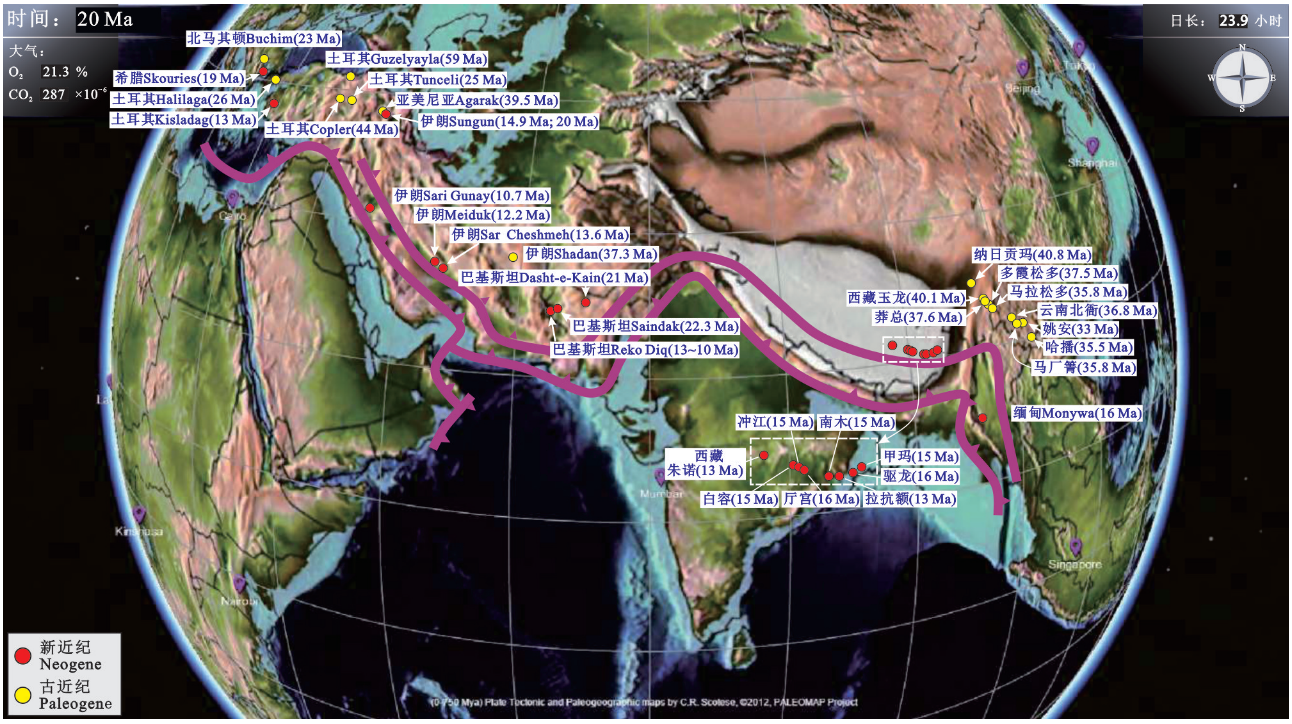

图 2　新特提斯洋后碰撞斑岩矿床的分布

（据张洪瑞等，2010；Richards，2015a；Wang et al.，2018；Yang et al.，2019；侯增谦等，2020a 修改）

Fig. 2　Distribution of post-collisional porphyry deposits in the Neo-Tethyan

(modified from Zhang et al., 2010; Richards, 2015a; Wang et al., 2018; Yang et al., 2019; Hou et al., 2020a)

集中于 41~39 Ma（Li et al.，2018；Htut et al.，2020）；④ 三江斑岩 Cu-Au 成矿带位于青藏高原东南缘，是中国最重要的有色金属与贵金属新战略基地之一。带内矿床近南北向分布，受印度—欧亚碰撞应力转换控制，发育一系列新生代断裂、富碱斑岩和与之相伴的多金属矿床，由北西向南东形成了由玉龙斑岩 Cu-Mo 矿、北衙斑岩-矽卡岩型 Au 多金属矿、马厂箐斑岩 Cu-Mo-Au 矿、姚安浅成低温热液-斑岩型 Pb-Ag-Au 多金属矿、哈播斑岩 Cu 多金属矿、长安冲斑岩 Cu 多金属矿（Hou et al.，2003b；毕献武等，2005；梁华英等，2009；Deng et al.，2014；2015；2021）等组成的多金属成矿区，被认为是中国重要的斑岩 Cu-Mo-Au 成矿省和成矿远景区之一，是中国 Cu-Au 多金属资源的重要产地，这些矿床的成矿年龄集中于 43~32 Ma。

值得指出的是，特提斯成矿域大规模斑岩成矿作用集中于后碰撞阶段（Hou et al.，2015b；2015c；2019；Wang et al.，2020），其成因机制尚存争议。有学者认为可能的原因为：① 古特提斯洋盆普遍缺氧，导致弧岩浆相对还原，不利于斑岩成矿（Richards et al.，2017）；② 新特提斯构造域油气资源丰富，导致俯冲过程的氧逸度偏低，无法满足斑岩成矿条件。而后碰撞阶段，随着俯冲下去的有机物被分解释放，氧逸度逐渐升高，俯冲阶段积累的成矿物质得以活化富集，有利于斑岩矿床的形成（Sun et al.，2017；孙卫东等，2020）。

1.4　中国斑岩矿床

斑岩型矿床对中国矿业具有重要意义，自 20 世纪 60 年代以来，中国地质学家对其展开大量的研究工作，对其时空分布进行了详细总结。研究表明，中国斑岩型 Cu 矿床主要分布在冈底斯带、玉龙带、中甸带、长江中下游带、中亚造山带、哀牢山—红河带以及多龙、德兴、铜矿峪等矿集区（图 3，Yang et al.，2019），形成于古元古代（~2100 Ma）、奥陶纪（~480~440 Ma）、石炭纪（~330~310 Ma）、晚三叠世—早白垩世（~215~105 Ma）以及始新世—中新世（~40~14 Ma）等 5 个时期，且主要集中于后 2 个时期（Yang et al.，2019）。成矿期次主要为：华力西期（石炭纪—二叠纪，甘蒙北山带主要形成期）、印支期（义敦岛弧南段格咱岛弧斑岩 Cu 矿带）、燕山期（滨太平洋斑岩

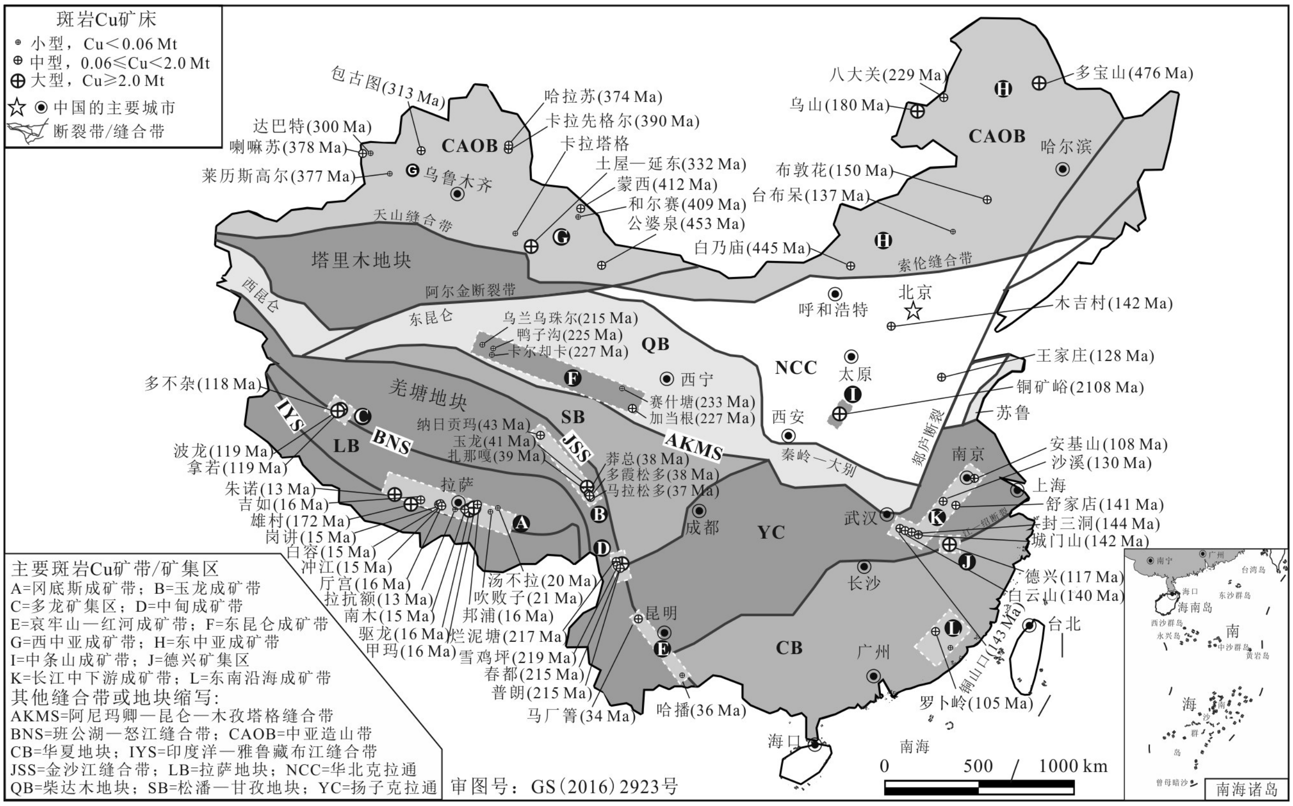

图3　中国斑岩铜矿床的分布及形成年龄(据Yang et al., 2019修改)

Fig.3　The distribution and mineralization ages of porphyry Cu deposits in China (modified from Yang et al., 2019)

Cu矿带、班公湖-怒江斑岩Cu矿带)和喜马拉雅期(冈底斯斑岩Cu矿带、扬子西缘斑岩Cu矿带)等4个主要成矿期(李文昌等, 2014)。

中国斑岩矿床与全球3大成矿域在时空分布规律上具有良好的对应性(图1),但时间序列和形成环境有其独特性和复杂性(李文昌等, 2014)。中国斑岩矿床成矿时代因产出地不同,时代跨度较大,但各成矿带成矿环境的一致性和时空分布规律性较强(图3、4,表1)。如西藏玉龙成矿带、哀牢山-红河成矿带形成于碰撞造山环境的构造转换阶段,形成时代集中在43~32 Ma,西藏冈底斯成矿带则形于碰撞造山环境的地壳伸展阶段,成矿主要集中在20~10 Ma,均属喜马拉雅期。

除斑岩Cu矿外,中国还发育斑岩Mo矿。中国斑岩型Mo矿床主要分布在秦岭-大别、兴-蒙、长江中下游、华南、青藏高原和天山-北山等6个主要Mo成矿带,形成于早古生代(480~420 Ma)、晚古生代(412~260 Ma)、中生代印支期(251~209 Ma)、中生代燕山期(194~77 Ma)和新生代(65~13 Ma)等5个时期,且主要集中于后2个时期(范羽等, 2014;黄凡等, 2014)。其中,秦岭-大别斑岩Mo矿带是世界著名斑岩Mo矿带,也是中国最为重要的Mo资源基地,目前控制储量约占全国总储量的50%(Li et al., 2012)。130~170 Ma是中国斑岩型Mo矿床成矿作用的主要发育时段(范羽等, 2014)。

2　产出构造环境

素有“俯冲带工厂”之称的岩浆弧(岛弧和陆缘弧)是产出巨型斑岩Cu矿的重要环境(Richards, 2003; 2013; Cooke et al., 2005)(图1)。如前文所述,岛弧斑岩Cu矿以环西太平洋斑岩Cu矿带为代表(Harrison et al., 2018; Maryono et al., 2018),典型矿床包括菲律宾的Far South East和Atlas Cu-Au矿床、印度尼西亚的Batu Hijau和Tumpanpitu Cu-Au矿床等;陆缘弧斑岩Cu矿以南美安第斯斑岩Cu矿带为代表(Cox et al., 2020),典型矿床包括阿根廷Bajo de la Alumbera Cu-Au矿床和智利El Teniente Cu-Mo矿床等。这些大型、超大型斑岩矿床常成群出现,表明产出斑岩矿床的岩浆弧环境具有特殊的动力学背

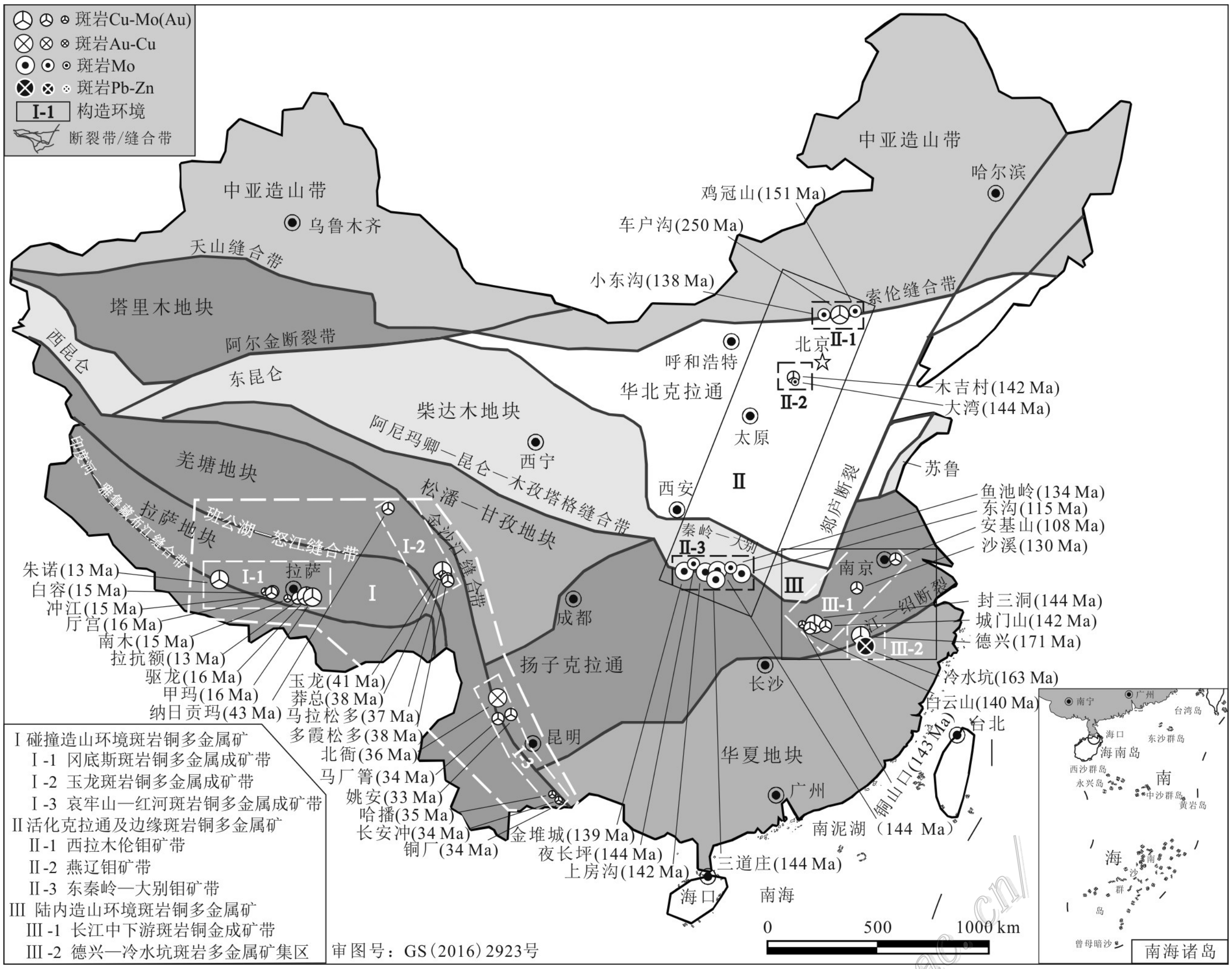

图4　中国大陆非弧环境斑岩型矿床分布及年龄(据Yang et al.,2019;侯增谦等,2020a修改)

Fig.4　The distribution and mineralization ages of non-arc porphyry deposits in Chinese mainland (modified from Yang et al., 2019; Hou et al., 2020a)

景和(或)地壳结构。有学者指出汇聚板块边缘的挤压构造背景对形成斑岩矿床具有重要作用(Sillitoe, 1998),而大洋板片的低角度俯冲是形成挤压背景的有利条件(Cooke et al.,2005)。但是长期持续的挤压背景却不利于斑岩型矿床的形成,而由挤压向伸展转换(Richards,2003)、俯冲角度变化(James et al., 1999)等构造机制转换阶段(Kerrich et al.,2000; Richards,2003;Cooke et al.,2005),常被视为控制斑岩型矿床形成的有利因素。

近年来,国内外学者基于大地构造背景、岩浆岩岩石学和地球化学、成矿规律等多学科综合研究,提出斑岩型Cu矿床还可以产于与俯冲无关的陆-陆碰撞环境(Hou et al., 2009; 2015b)和大陆陆内环境(Hou et al.,2004;2015d;胡瑞忠等,2015)。前者以青藏高原玉龙斑岩Cu矿带和冈底斯斑岩Cu矿带以及伊朗高原Kerman-Arasbaran巨型斑岩Cu矿带为代表;后者以华南地区斑岩Cu矿和长江中下游斑岩Cu-Au成矿带等为代表(图1~3)。由此构建了碰撞造山环境、陆内造山环境斑岩Cu矿成矿模式(Hou et al., 2009; 2015b; 2019; Yang et al., 2009; 侯增谦等,2009;2011),取得了斑岩成矿理论上的突破。特别是,碰撞造山环境斑岩Cu矿成矿模式不仅丰富了世界斑岩Cu矿床的研究,而且进一步指导和推动了诸如冈底斯斑岩Cu矿带等的找矿重大突破。随着研究的深入,一大批地质年代学和地球化学资料涌现(Hou et al., 2003b; 2015a; Qu et al., 2007; Wang et al., 2014; Yang et al., 2015)。前人根据这些资料,总结出产于各类构造环境的大型斑岩Cu矿均见于中

表 1 中国大陆非弧环境斑岩型矿床成矿岩浆起源

Table 1 Origin of ore-forming magmas for non-arc porphyry deposits in Chinese mainland

<table>
<tr><th colspan="2">构造环境</th><th>典型矿床</th><th colspan="2">成矿斑岩岩浆起源</th><th>资料来源</th></tr>
<tr><td rowspan="4">碰撞造山环境</td><td rowspan="2">构造转换阶段</td><td rowspan="2">玉龙始新世斑岩成矿带、哀牢山—红河斑岩成矿带</td><td rowspan="4">岩浆起源具有相似性</td><td>俯冲大洋板片重融</td><td>Qu et al., 2004; 2007; Hu et al., 2017; Sun et al., 2018</td></tr>
<tr><td>俯冲板片熔体交代的地幔楔</td><td>Gao et al., 2007; 2010</td></tr>
<tr><td rowspan="2">地壳伸展阶段</td><td rowspan="2">冈底斯中新世斑岩成矿带</td><td>岩石圈地幔熔融</td><td>Lu et al., 2015</td></tr>
<tr><td>加厚的镁铁质新生下地壳部分熔融</td><td>Hou et al., 2013a; 2015b; 2017; 2019; Guo et al., 2007; Yang et al., 2015; Wang et al., 2018</td></tr>
<tr><td rowspan="7">陆内造山环境</td><td rowspan="3">岩石圈伸展阶段</td><td rowspan="3">德兴斑岩Cu矿床</td><td colspan="2">俯冲的古太平洋板片及其沉积物部分熔融</td><td>Zhou et al., 2000; Zhou et al., 2012</td></tr>
<tr><td colspan="2">拆沉的下地壳部分熔融</td><td>Wang et al., 2006</td></tr>
<tr><td colspan="2">新生的镁铁质下地壳部分熔融</td><td>Hou et al., 2013b</td></tr>
<tr><td rowspan="4">造山带崩塌阶段</td><td rowspan="4">长江中下游斑岩成矿带</td><td colspan="2">洋脊俯冲熔融</td><td>孙卫东等, 2008; Ling et al., 2009</td></tr>
<tr><td rowspan="3">下地壳熔融</td><td>加厚古老下地壳直接部分熔融</td><td>张旗等, 2001; 2002</td></tr>
<tr><td>底侵玄武质下地壳部分熔融</td><td>王强等, 2001</td></tr>
<tr><td>拆沉下地壳部分熔融</td><td>Xu et al., 2002; 王强等, 2004; 侯增谦等, 2007</td></tr>
<tr><td rowspan="2">活化克拉通边缘及内部</td><td rowspan="2">克拉通破坏阶段</td><td rowspan="2">木吉村斑岩Cu(Mo)矿床</td><td colspan="2">下地壳熔体与岩石圈地幔反应</td><td rowspan="2">Chen et al., 2004; 2008; Yuan et al., 2006; Gao et al., 2013</td></tr>
<tr><td colspan="2">交代富集的岩石圈地幔熔融</td></tr>
</table>

国大陆(图4,Kusky et al.,2007),这些矿床除少量产于岩浆弧外,主要产于碰撞造山环境的构造转换和地壳伸展阶段、陆内造山环境的岩石圈伸展和崩塌阶段以及活化克拉通的边缘及内部(图4,侯增谦等,2020a)。进一步总结发现,中国超过一半的斑岩Cu矿形成于碰撞造山环境(Hou et al.,2004;2009;Yang et al.,2009;2016),而不是在大多数斑岩Cu矿典型的陆缘弧或岛弧环境中(Cooke et al.,2014)。由此可见,以冈底斯中新世斑岩Cu-Mo成矿带、玉龙斑岩Cu成矿带等为代表的碰撞造山环境斑岩Cu矿在中国占有重要地位。

3 成矿斑岩成因与成矿动力学机制

弧斑岩型矿床通常形成于俯冲带上方的岛弧(图5a)或陆缘弧(图5b)环境,成因上与洋壳俯冲密切相关,尤其是与板片部分熔融或俯冲板片脱水触发地幔物质部分熔融密切相关(Richards, 2003; Cooke et al., 2005; Sillitoe, 2010; 2018; Wilkinson, 2013;图5a、b),成矿斑岩主要为钙碱性系列,主要岩相为花岗闪长岩、石英闪长岩、石英二长岩,地球化学特征多表现出高Sr/Y和La/Yb的埃达克岩属性(如洋脊俯冲、平板俯冲和成熟大陆弧环境中成矿斑岩)(Singer et al., 2005; Richards et al., 2007; 2012; Zhang et al.,2017)。大量研究表明,俯冲带斑岩Cu矿的形成经历了以下过程:① 俯冲板片的脱水或部分熔融并交代地幔楔诱发橄榄岩部分熔融;② 地幔岩浆上升至下地壳底部并经历熔融—同化—储存和均一化(MASH)以及初期分离结晶;③ 初始母岩浆自下地壳底部上升至中上地壳底部形成岩浆房;④ 岩浆侵位与挥发分出溶;⑤ 成矿流体形成、运移、汇集与最终的金属沉淀等(Richards,2003;2011;Sillitoe,2010;Wilkinson,2013;毛景文等,2014;Sun et al.,2015;Zheng et al.,2016;Zhang et al.,2017;Chen et al.,2020)。在此过程中,大洋岩石圈板块俯冲无疑是导致弧岩浆作用和斑岩Cu矿形成发育的根本性动力学机制(Richards,2003;2011),大洋板片携沉积物俯冲和深部脱水造就了富水、高S和高氧逸度环境,使得深部金属以硫酸盐相被迁移而带入到浅部成矿系统(Richards,2003;Cooke et al.,2014)。而洋脊俯冲(Cooke et al.,2005;Sun et al.,2011)、俯冲板片撕裂(Kerrich et al.,2000;Hou et al.,2009)、俯冲角度变化(Kay et al.,2001)与俯冲极性翻转(Kerrich et al.,2000)等过程,常被视为控制地幔源区熔融、岩浆形成演化、岩浆-热液系统发育及斑岩成矿系统形成的有利因素。

对于非弧斑岩型矿床,不论是在大洋板片俯冲早已停止的碰撞造山带和板内环境,还是在俯冲板片前缘未必能到达成矿岩浆源区的陆内造山带或崩塌环境,成矿岩浆直接来自俯冲洋壳板片熔融的可

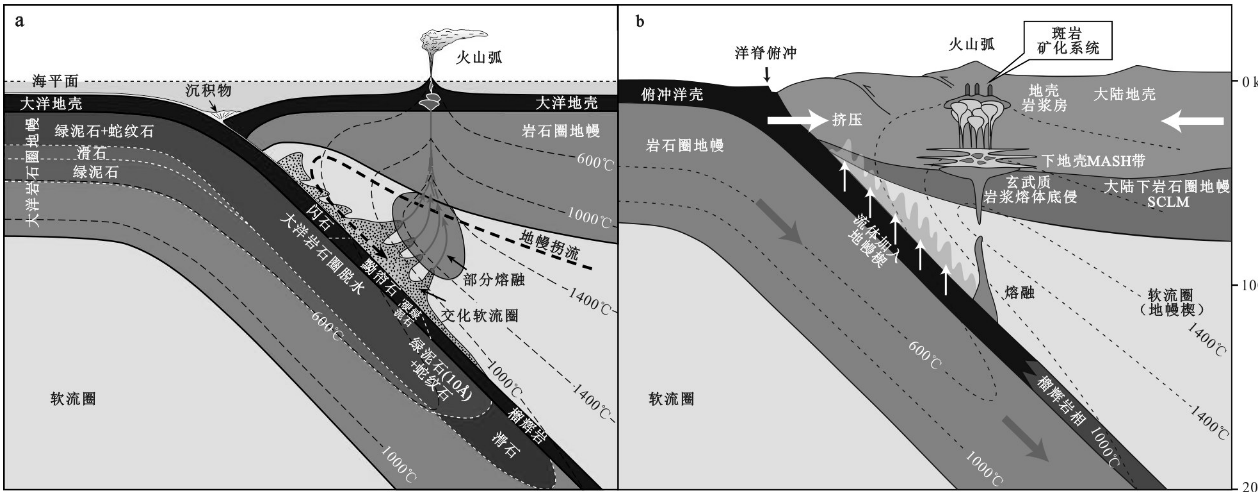

图5　俯冲带岛弧(a,据Richards,2011)和陆缘弧(b,据Wilkinson,2013)环境斑岩铜矿有关岩浆起源模型和斑岩铜矿成矿过程的示意图

Fig. 5　Model of magma origin for island arc setting (a, after Richards, 2011) and continental margin arc setting (b, after Wilkinson, 2013) and schematic diagram for porphyry copper mineralization in subduction zone

能性较小(Hou et al.,2011)。该类矿床成矿斑岩多为高钾钙碱性系列,主要岩相为石英闪长岩、二长花岗岩、花岗岩,少量为钾玄质系列,以高钾为特征(侯增谦等,2007;Yang et al.,2019),通常显示埃达克岩地球化学亲和性(张旗等,2001;Xu et al.,2002;Wang et al.,2006;Hou et al.,2009;2013a;2013b;Aghazadeh et al.,2015)。前人对这类斑岩矿床中成矿岩浆的来源进行了深入研究,提出了不同的成因观点(表1)。由于地质过程的复杂性,部分观点尚存争议。有学者综合最新研究成果(典型矿床的地质、地球化学、地球物理探测等)对不同成因理论进行分析总结,认为产于中国大陆非弧环境的成矿斑岩,主要起源于加厚的镁铁质新生下地壳或拆沉的古老下地壳,少数起源于遭受早期俯冲板片流体/熔体交代改造过的富集地幔(侯增谦等,2020a)。导致这些源区部分熔融的主要诱发机制包括大陆碰撞和陆内俯冲引起的地壳大规模增厚和紧随其后的板片撕裂(Liu et al.,2020;Luo et al.,2022;Wang et al.,2022)或断裂(Zheng et al.,2019)、断离(Williams et al.,2004;Pan et al.,2012;Wang et al.,2015;Zhu et al.,2015)、岩石圈拆沉(Turner et al.,1996;Chung et al.,2005)和软流圈上涌等(侯增谦等,2020a)。基于上述认识构建了非弧环境斑岩Cu矿岩浆起源模型(图6),为中国大陆非弧环境成矿斑岩成因提出了合理的解释。

陆-陆碰撞环境斑岩型矿床有别于经历洋壳俯冲、沉积物脱水交代地幔楔等一系列深部过程的弧斑岩型矿床,其形成经历了以下过程:① 大陆碰撞导致新生下地壳(俯冲改造的下地壳+部分岩石圈地幔)部分熔融;② 埃达克质岩浆上侵形成大的岩浆房;③ 岩浆房流体出溶形成斑岩矿床(侯增谦等,2004a;2004b;陈衍景等,2009;杨志明等,2009);相比之下,陆内造山环境斑岩型矿床所产出的构造环境和形成的动力学背景还尚存争议,目前较为合理的解释为:① 经历强烈陆内俯冲和地壳加厚的岩石圈因软流圈上涌而伸展,诱发新生下地壳熔融,产生岩石圈伸展阶段富Cu-Au岩浆;② 岩石圈拆沉导致下地壳熔融,其熔体与上覆交代富集的地幔岩发生反应,产生造山带崩塌阶段富Cu-Fe-Au岩浆(图6c,d)。

值得关注的是,这两类构造环境下成矿斑岩地球化学对比研究发现,不论是岩浆弧还是非弧环境,成矿斑岩常显示出类似的弧岩浆地球化学特征,如相对富集LILE(如K、Ba、Sr等),相对亏损HFSE(如Nb、Ta、Ti、P等)(侯增谦等,2004a;王强等,2004;Hou et al.,2004;Jiang et al.,2006;Wang et al.,2006;Richards,2009;2011),暗示两类环境的岩浆源区具有内在的成生联系和继承关系(Hou et al.,2009;2015b;Richards,2009)。这种现象在特提斯成矿域尤为明显,特别是冈底斯带内俯冲和碰撞型矿床的时空分布显示了这种相关性(Hou et al.,2015b;Wang et al.,2017)。因此,有理由相信大陆碰撞之前

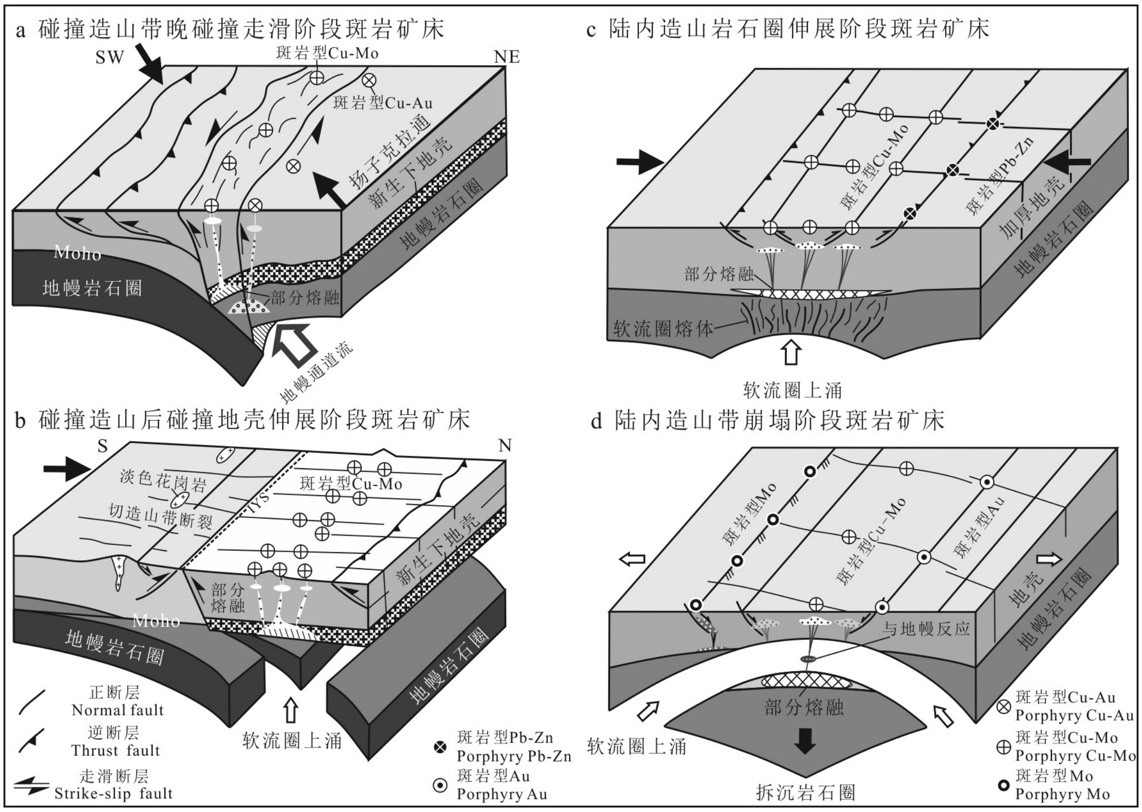

图6 非弧环境斑岩矿床岩浆起源和动力学背景示意图(据Hou et al.,2011)

a. 碰撞期大洋板片流体交代的楔形地幔和弧岩浆底侵形成的新生下地壳发生部分熔融,分别形成含Cu-Au和Cu-Mo岩浆,其侵位受大规模走滑断裂活动控制;b. 碰撞前的弧岩浆在地壳底部底侵形成新生下地壳(含硫化物和含水堆积带),其部分熔融和硫化物分解形成含Cu-Mo岩浆,并在横切碰撞带正断层系统的控制下侵位;c. 经历强烈陆内俯冲和地壳加厚后的岩石圈因软流圈上涌而伸展,诱发镁铁质弧岩浆底侵体(新生下地壳)熔融,产生富Cu-Au岩浆;d. 岩石圈拆沉导致下地壳熔融,其熔体与上覆的交代富集的地幔岩(地幔橄榄岩)发生反应,产生富Cu-Fe-Au岩浆

Fig. 6 Schematic diagram of magma origin and dynamic setting for non-arc porphyry Cu deposits (after Hou et al., 2011)

a. During the collision period, melting of the mantle wedge metasomatized by oceanic plate fluids and the juvenile lower crust formed by the under-transgression of arc magma, forming the Cu-Au and Cu-Mo magmas respectively, and their emplacement was controlled by large-scale strike-slip faults; b. Before the collision, the arc magma was emplaced at the bottom of the crust to form the juvenile lower crust (sulfide and water-bearing accumulation zone), and its partial melting and sulfide decomposition formed Cu-Mo magma, which was emplaced under the control of the normal fault system in the crosscutting collision zone; c. After intense intracontinental subduction and crustal thickening, the lithosphere was extended due to asthenosphere upsurge, which induced the emplacement melting of mafic arc magma (juvenile lower crust) and produced Cu-Au rich magma; d. Lithospheric delamination leads to the melting of the lower crust, which reacts with the metasomatic and enriched mantle rocks to produce Cu-Fe-Au rich magma

的洋壳俯冲作用为活动大陆边缘碰撞成矿提供了先决条件(水、S和金属元素等)(Richards,2009;Wang et al.,2018;Zheng et al.,2019)。

4 成矿金属来源

斑岩成矿系统中成矿物质(包括Cu、Mo、Au等成矿金属,以及S、Cl和水等挥发分)的最终来源包括俯冲洋壳、上部地幔以及地壳3种地质端员。

岩浆弧下地幔包体的研究表明,俯冲板片流体交代地幔楔形成的含金属辉石岩脉,比周围未被交代的橄榄岩富集了2~800倍不等的Cu、Au和PGE(McInnes et al.,1999),而俯冲带的Os和O同位素研究揭示俯冲洋壳对于亲铜元素的贡献比例低于10%,指示Cu、Au等可能源于地幔而非俯冲板片熔体,板片流体交代作用促使成矿金属元素在地幔楔中再分配和再富集(McInnes et al.,1999;Griffin et al.,2013)。因此,俯冲带岩浆弧环境中成矿金属主

要来源于俯冲板片流体交代地幔楔,后者部分熔融使金属元素被释放到弧岩浆系统中,形成斑岩矿床(Pettke et al.,2010;Richards,2011;2015b)。

对于非弧斑岩型矿床,不同构造环境下成矿金属来源不尽相同:① 碰撞造山环境(如冈底斯带),早中生代冈底斯幔源弧岩浆在地壳底部大规模底侵固结,局部发生堆晶(如堆晶角闪岩,Cu:~1000×10^{-6},Xu et al.,2019),形成富含金属硫化物的新生镁铁质下地壳(辉长岩及石榴子石角闪岩,发育岩浆成因原生Cu硫化物,Zhang et al.,2014)。碰撞期该新生下地壳重熔或分解,为岩浆提供大量的金属Cu(Richards et al.,2009;Hou et al.,2009;2013a;2015b;2019)。带内成矿斑岩(δ^{65}Cu=0.18‰~0.87‰)和热液黄铜矿(δ^{65}Cu=0.08‰~1.01‰)较贫矿斑岩(δ^{65}Cu=−0.04‰~+0.18‰)明显富集重δ^{65}Cu同位素,同样证明成矿岩浆和金属源自硫化物富集的新生下地壳而非地幔(δ^{65}Cu=0.03‰±0.24‰)(Zheng et al.,2019);② 陆内造山带或板内环境,拆沉下地壳熔融产生的熔体(通常因榴辉岩化过程而贫金属,Cameron,1989)与金属再富集的岩石圈地幔(如板片流体交代的楔形地幔)反应,并从后者萃取金属Cu(Au),形成含矿斑岩岩浆(Hou et al.,2011);③ 金属Mo则主要来自具有高Mo丰度大陆地壳熔融的长英质岩浆(Sinlair,2007;Klemm et al.,2007;Hou et al.,2011)。

研究表明,不论在岩浆弧还是非弧环境,成矿岩浆通常相对富集成矿金属(Cu、Au、Mo),但斑岩矿床的形成并不要求成矿岩浆在初始阶段就异常富集金属组分(Cline et al.,1991),但要求金属硫化物相在岩浆流体出溶前没有发生大规模的饱和及分离,而该过程又受岩浆氧逸度和含水量等控制(Candela et al.,2005;侯增谦等,2020a)。

5　蚀变-矿化分带模式

斑岩矿床具有典型的蚀变分带特征。早在20世纪70年代,Lowell等(1970)就提出了一直沿用至今的经典的俯冲型斑岩Cu矿床蚀变分带模式,即从岩体中心向外表现为:钾硅酸盐化(钾长石-黑云母-石英等)→绢英岩化(绢云母-石英-黄铁矿等)→(泥化)→青磐岩化(绿泥石-绿帘石-方解石等)的水平蚀变带(图7a)。在此模式中,Cu矿化主要发生于钾化带和绢英岩化带及2者之间的过渡部位,并伴随不同程度的辉钼矿化,同时绢英岩化带也发育较强黄铁矿化;青磐岩化带或围岩中可能发生浅成低温热液成矿作用,形成Pb、Zn、Ag、Au矿化等(张洪涛等,2004)。成矿过程中,当围岩是碳酸盐岩,成矿流体与围岩相互作用,在接触带可以形成矽卡岩型Cu多金属矿床,沿层交代出现Cu-Pb-Zn矿;在浅部形成脉状Pb-Zn-Ag矿以及低温热液脉型Au-Ag-Sb-Hg矿(Sillitoe,2010;毛景文等,2014)。地质学家在研究南美洲和西南太平洋的斑岩Cu矿床中发现,早期钾硅酸盐化被晚期绢英岩化蚀变所叠加和覆盖,绢英岩化蚀变带通常发生在钾硅酸盐化带内,而不是在钾硅酸盐化带周围(图7a,Gustafson et al.,1975)。随后,学者们越来越清楚地认识到,斑岩Cu矿早期蚀变(如钾化和青磐岩化)主要受斑岩侵入体的形状控制,而最终蚀变特征主要取决于构造背景和蚀变叠加程度。俯冲型斑岩Cu矿床中的Cu等金属元素主要沉淀于钾硅酸盐化阶段,含Cu矿物主要为蓝辉铜矿及斑铜矿(图7b,Lowell et al.,1970;Sillitoe,2010)。

然而,经典的蚀变与矿化模型显然难以解释碰撞造山环境斑岩型Cu矿床,该类矿床在蚀变分带与矿化分带上呈现出某些特定的蚀变组合及分带特征。以青藏高原碰撞环境斑岩Cu矿为代表,绢英岩化强烈叠加于钾硅酸盐化之上,而非围绕其外围,且中国超过一半的超大型斑岩Cu矿床的Cu矿化主要发生在绢英岩化阶段,特别是绿泥石-绢云母阶段,而非通常认为的钾硅酸盐化阶段,矿石矿物主要为黄铜矿和黄铁矿(图7b)。由此,杨志明等(2009)、Yang等(2014;2019)在详细总结中国主要斑岩铜矿床的蚀变特征的基础上,建立了碰撞型斑岩铜矿床蚀变与矿化分带模型(图7a),并且认为导致绢英岩化强烈叠加在早期钾硅酸盐化带内的原因与中国碰撞造山带斑岩Cu矿及区域普遍都经历了同矿化期较高的构造抬升速率有关(Yang et al.,2019)。这些发现和认识均有别于经典的俯冲带斑岩型Cu矿床,是对经典斑岩蚀变与矿化模型的重要补充和完善。

6　斑岩成矿的控制因素

斑岩型矿床的形成离不开3个关键过程:① 岩浆在出溶流体之前就具有成矿潜力,且在演化过程中有能力发生流体出溶;② 出溶的成矿热液能够运移到成矿有利部位;③ 成矿热液在物理化学条件改变的情况下,发生成矿金属元素的沉淀富集。因此,

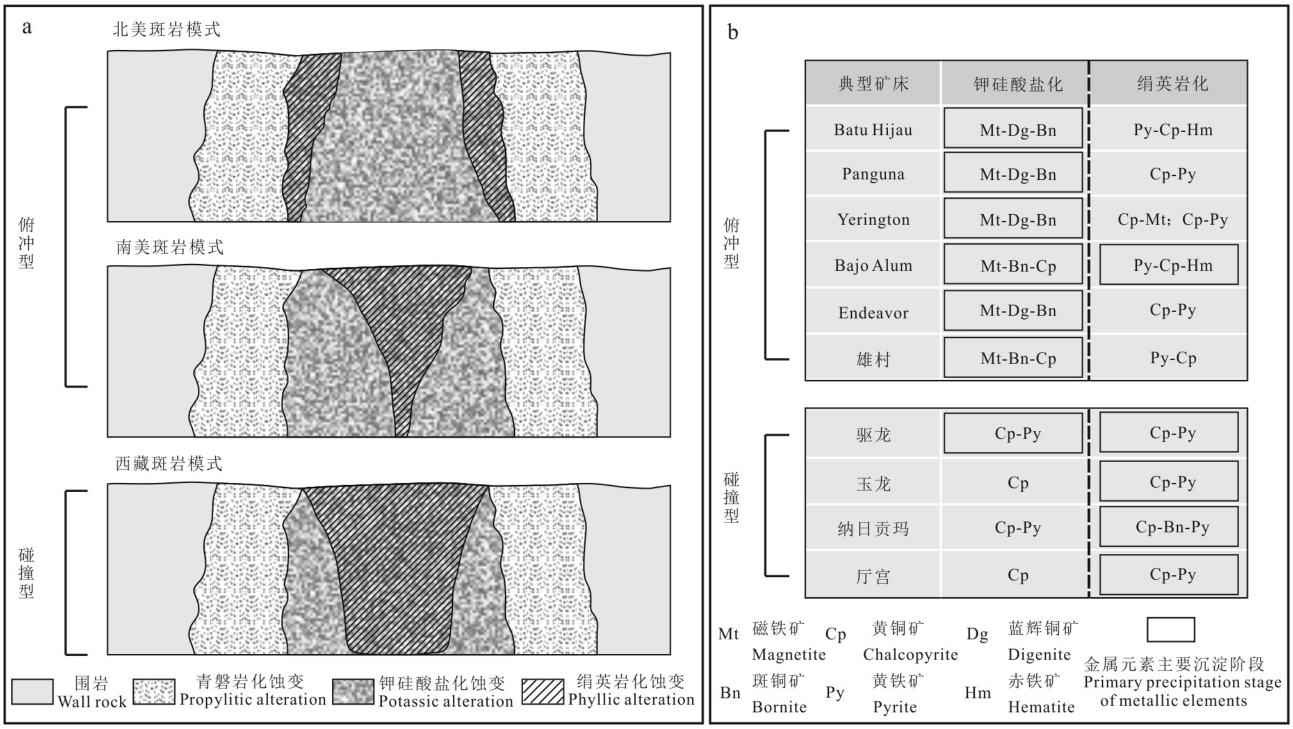

图 7 斑岩 Cu-(Mo-Au)矿床热液蚀变分带模式图(a)和矿物组合及矿化阶段(b)(据 Yang et al.,2019)

Fig. 7 Hydrothermal alteration zoning patterns(a), mineral assemblages and mineralization stage (b) for porphyry Cu (-Mo-Au) deposits (after Yang et al.,2019)

岩浆能否形成具有成矿潜力的岩浆热液及迁移、富集成矿过程，是形成斑岩型矿床的关键环节(Richards,2015b)。大型斑岩矿床的形成需要岩浆具有较高的氧逸度、水含量以及 S、Cl 等挥发分元素(Richards, 2003; Sillitoe, 2010; Wang et al., 2018; 2020; Xu et al.,2021)，因此，限定斑岩岩浆系统中熔体的氧逸度、水含量和挥发分组成，并解析其演化的影响因素，成为约束斑岩矿床成矿岩浆条件及其演变过程的重要内容。此外，斑岩型矿床的形成需要许多有利条件的高度耦合，或是需要某些特殊条件，如源区性质、岩浆性质(氧逸度、含水量、挥发分等)、岩浆混合作用等，这些因素或作用对斑岩成矿的影响和贡献值得深入探讨。

6.1 岩浆源区

岩石圈尺度的深部构造和地质过程演化控制着大型成矿系统的形成发育和空间分布(Kerrich et al.,2000;Hou et al.,2015c)，如冈底斯成矿带内斑岩 Cu 矿床严格地限制于南、北拉萨地体之内，与新生地壳分布区相对应，矽卡岩型 Fe(-Cu)和 Pb-Zn 矿床及其成矿带严格地限定在中拉萨地体及其边界带，与古老地壳和再造地壳相对应(侯增谦等,2018)。而岩浆源区性质、演化及地质过程等对斑岩型矿床的形成起到关键控制作用，主要表现在：① 岩浆源区壳幔组分的富集程度对矿化元素具有一定的制约，如少量幔源物质的加入有利于形成含 Cu 或含 Mo 的岩体，而新生地壳组分的加入有利于形成含 Au 岩体(Lu et al.,2013)；② 岩浆源区受流体交代程度的高低会导致斑岩—矽卡岩型矿床形成不同的金属矿化，如低程度流体交代形成的岩浆容易形成 Mo(-Cu)矿化，而高程度流体交代形成的岩浆容易发生 Cu-Mo(-Au)矿化(杨志明等,2008)；③ 成矿金属元素在源区的预富集能有效提高该富集金属硫化物地壳部分熔融形成的岩浆的成矿潜力(Hou et al., 2015b;Zheng et al.,2019;Wang et al.,2020)；④ 源区岩浆演化过程中岩浆的全碱含量(Na_2O+K_2O)也对矿化元素具有一定制约(Lu et al.,2013)，如 Cu、Mo 矿化与亚碱性或高钾钙碱性岩浆有关，而 Au 矿化多与具有较高的 Na_2O+K_2O 和 K_2O/Na_2O 的碱性岩浆有关，高 K^+ 能够提高 Au 在熔体中的溶解度(Zajacz et al.,2010)。

地壳物质组成(如新生地壳/古老地壳/再造地壳)、深部地质过程(如岩石圈拆沉、岩浆底侵/热蚀、

地壳减薄/加厚等)及地球动力学背景(如俯冲造山、碰撞造山、陆内造山、板内构造等)等都在一定程度上控制了成矿母岩浆的构造-岩浆组合和岩石地球化学特征(侯增谦等,2018)。因此,岩浆源区具有一定复杂性。而近年来随着同位素地质学的发展,Hf-Nd同位素为解决岩石源区问题,提供了很好思路。全岩 $\varepsilon_{Nd}(t)$ 和 T_{DM2} 可以用于区分岩浆的可能来源和地壳源岩的形成年龄(侯增谦等,2018),而锆石 $\varepsilon_{Hf}(t)$ 值可用于识别新生地壳($\varepsilon_{Hf}(t)>0$)和古老地壳($\varepsilon_{Hf}(t)<0$)(Kemp et al.,2006)。因此,岩浆岩Hf-Nd同位素可以效示踪岩石的源区特征、成分与性质和追溯岩石圈及地壳形成演化。区域尺度的Hf-Nd同位素填图,则可整体探测造山带和克拉通岩石圈物质结构,精细刻画不同地壳块体深部物质组成和时空分布,并深刻揭示深部致矿过程和区域成矿规律(侯增谦等,2018;2020b;Luo et al.,2022)。

6.2　岩浆氧逸度

不论是俯冲还是碰撞背景下的斑岩矿床,成矿岩浆都具有显著的高氧逸度特征($\Delta FMQ>1.5$)(Richards,2003;2011;2015a;Wang et al.,2014)。氧逸度是斑岩矿床诸多控矿因素之中极其关键的一个,在岩浆演化过程中,氧逸度能通过控制变价元素的价态(如:Fe、Cu、Au、V、S等),影响这些元素在岩浆中的溶解度和赋存状态(Richards,2011;Wang et al.,2014),进而控制矿床的形成。主要表现为:① 还原条件下,S主要以 S^{2-} 的形式存在,当硫化物的溶解度达到饱和时,Cu及其他亲铜元素将从熔体中分离(Jugo et al.,2005;Lee et al.,2012)。因此,如果岩浆源区的氧逸度较低,Cu、Au金属元素容易在岩浆结晶分异过程中在地壳深部发生堆积而不是随着熔体上升到地壳浅部(Richards,2009;Lee et al.,2012);② 高氧逸度条件下,岩浆中S主要以 SO_4^{2-} 和 SO_2 的形式溶解于硅酸盐熔体中,抑制了 S^{2-} 与Au、Cu、Mo等金属阳离子结合形成硫化物,使得熔体中金属硫化物含量较低,无法达到饱和(Sun et al.,2013;2015),最终有利于Au、Cu、Mo等亲铜元素逐渐富集到残余岩浆并进入流体相而运移至浅部富集成矿(Jugo,2009;Sun et al.,2015;Richards,2015b)。研究表明,斑岩岩浆氧逸度高于 $\Delta FMQ+1.5$ 是成矿的关键(Sun et al.,2013;2015;2017;Zhang et al.,2017),而氧逸度的上限为HM缓冲剂(Sun et al.,2015)。此外,不论是以智利Chuquicamata—EI Abra斑岩Cu矿带为代表的俯冲环境,还是以冈底斯斑岩Cu矿带为代表的碰撞环境,抑或是以德兴斑岩Cu矿为代表的陆内造山环境,成矿岩浆均比非成矿岩浆具有更高的氧逸度(Ballard et al.,2002;Wang et al.,2014;Zhang et al.,2017;Zheng et al.,2020)。

由此可见,岩浆氧逸度的估算对揭示斑岩矿床金属富集成矿的关键过程和成矿潜力研究均具有重要意义。前人关于岩浆氧逸度的估算方法已有一定积累(表2),为选择合适的方法以获取更能反映真实情况的数据提供了依据。同时,从表中可以看出,作为岩浆岩的副矿物,锆石、磷灰石等在岩浆氧逸度估算中展现出广阔的应用前景。

6.3　岩浆含水量

母岩浆富水亦是形成斑岩型矿床的关键(Lu et al.,2015;Richards,2015b;Williamson et al.,2016),含水量决定了岩浆流体能否饱和及出溶。岩浆形成过程中,较高的含水量(如镁铁质熔体)能够降低源区岩石的熔点,促进岩浆部分熔融,形成的高温岩浆能够降低源区Cu(Au)等金属硫化物的稳定性,使得早期残留于源区内的金属硫化物发生重熔,并且能够随着熔体向上运移(Wang et al.,2014)。富水岩浆侵位至浅部(3~6 km),高的初始含水量有利于岩浆在减压过程或者分离结晶过程中达到水饱和(Robb,2005),并使熔体中的水以流体的形式出溶(Yang et al.,2016),使Cu、Au等金属元素卸载、迁移并聚集成矿。

研究表明,不论是俯冲还是碰撞背景下的斑岩矿床,成矿岩浆都具有高的水含量(>4.5%,甚至高达10%)(Richards,2003;Wang et al.,2014;Lu et al.,2015)。

而近期有研究指出,并不是含水量越高越有利于成矿。Chiaradia(2020)采用蒙特卡罗法对全世界范围内的斑岩型Cu矿床的母岩浆水含量进行了模拟计算,结果显示,2%~6%是最有利于矿化的弧岩浆含水量范围。可见,岩浆含水量的估算对斑岩成矿潜力研究具有重要意义。相比氧逸度,岩浆水含量的估算要困难得多,学术界关于斑岩矿床成矿岩浆水含量的估算经历了早期定性描述(成矿岩浆富水或贫水)到后期定量分析的转变,常用的测算方法见表3。

6.4　S、Cl等挥发性组分

挥发性组分(H_2O、CO_2、卤族元素和S等)不仅可以作为岩浆的重要组成部分,直接或间接地影响到岩浆性质和岩浆作用过程,而且制约着元素在熔体/流体相中的分配,以及在流体中的地球化学行为

表 2　岩浆岩氧逸度常用估算方法

Table 2　Methods commonly used to estimate magmatic oxygen fugacity

<table>
<tr><th colspan="2">分类</th><th>基本原理</th><th>氧逸度定性评估或定量计算方法</th><th>适用性</th><th>数据来源</th></tr>
<tr><td colspan="2">标志矿物</td><td>矿物标型特征及指示意义</td><td>石英+榍石+磁铁矿+富镁角闪石组合指示岩浆 $\lg f(O_2)$>NNO+1
熔融包裹体中发育硬石膏子晶或斑岩体存在磁铁矿，均指示岩体具有高氧逸度；磁黄铁矿的出现指示岩体具有还原性</td><td>—</td><td>Audétat et al., 2004</td></tr>
<tr><td colspan="2">矿物化学平衡，如Fe-Ti氧化物组合</td><td>固相间Fe-Ti互扩散和熔体-氧化物之间Fe-Ti扩散控制了Fe-Ti氧化物成分的变化和再平衡，存在如下反应：$6FeTiO_3(Ilm)+2Fe_3O_4(Mt)=6Fe_2TiO_4(Usp)+O_2$（Usp、Mt代表钛磁铁矿固溶体中钛尖晶石和磁铁矿的含量，Ilm为钛铁矿固溶体中钛铁矿的含量）</td><td>Fe-Ti氧化物温度-氧逸度计：$\Delta G^0=-RT\ln Kp=-RT\ln f_{O_2}^{-1/4}$
（R为气体常数，ΔG^0由钛铁尖晶石、磁铁矿、钛铁矿和赤铁矿的生成自由能计算得来）</td><td>适用条件：① Fe-Ti氧化物和岩浆之间完全平衡；② Fe-Ti氧化物的成分从喷发前最后一个岩浆储库到地表完全冷凝过程中没有任何变化；局限性：只有喷发和降温都很快的岩浆系统（如Plinian式火山喷发）中形成的Fe-Ti氧化物才可能将岩浆房内的温度和氧逸度记录下来</td><td>Buddington et al., 1964；Ghiorso et al., 2008；Hou et al., 2021</td></tr>
<tr><td colspan="2">多价元素不同价态比值，如：全岩或火山玻璃或熔体包裹体$Fe^{3+}/\Sigma Fe$值</td><td>Fe受氧逸度影响发生氧化还原反应，形成Fe^{2+}、Fe^{3+}</td><td>氧逸度与$Fe^{3+}/\Sigma Fe$比值关系：$\ln\frac{XFe_2O_3}{XFeO}=a\ln f_{O_2}+\frac{b}{T}+c+\sum_i d_iX_i+e\left[1-\frac{T_0}{T}-\ln\left(\frac{T}{T_0}\right)\right]+f\frac{p}{T}+g\frac{(T-T_0)p}{T}+h\frac{p^2}{T}$
（$\frac{XFe_2O_3}{XFeO}$为岩石中Fe_2O_3与FeO成分的摩尔比，T为温度，T_0为参考温度，p为压力，X_i为主量元素的摩尔分数，a~h为实验常数）</td><td>局限性：$Fe^{3+}/\Sigma Fe$比值与矿物化学平衡反映的是岩浆或矿物相最后平衡时的氧化还原状态。而当岩浆离开源区后，结晶分异、地壳混染、岩浆去气等浅部过程将不同程度地改变岩浆的氧逸度</td><td>Kress et al., 1991；Zhang et al., 2016；Lanzirotti et al., 2018</td></tr>
<tr><td colspan="2">全岩微量元素比值，如V/Sc值</td><td>V在熔体和矿物间的分配受氧逸度控制，与其地球化学行为相似的非氧化还原依赖元素（如Sc）比值，可以估算岩浆源区的氧化还原状态</td><td>在一定温度下，岩浆氧逸度越高其V/Sc值越大</td><td>成岩后的风化和变质过程不会对V/Sc值产生影响</td><td>Canil, 2002；Li et al., 2004</td></tr>
<tr><td rowspan="3">多价元素矿物/熔体分配系数</td><td rowspan="2">磷灰石
δEu、δCe
$S^{6+}/\Sigma S$值</td><td rowspan="2">多价元素（如Mn、Eu、Ce、S）在磷灰石/熔体之间的分配系数受氧逸度控制</td><td>$\lg f(O_2)=-0.0022(\pm0.0003)Mn(\times10^{-6})-9.75(\pm0.46)$</td><td>适用条件：岩浆成分范围为钙碱性中酸性岩，是否应用于其他熔体还需进一步研究，温度范围为660~920℃</td><td>Miles et al., 2016</td></tr>
<tr><td>$S^{6+}/\Sigma S$值增大反映体系氧逸度升高；较高的δEu和较低的δCe、Ga含量可以反映较高的氧逸度</td><td>—</td><td>Konecke et al., 2017；冷成彪等, 2020</td></tr>
<tr><td>锆石
Ce^{4+}/Ce^{3+}
Ce_N/Ce_N^*
Eu_N/Eu_N^*</td><td>多价元素（如Ce、Eu）在锆石/熔体之间的分配系数受氧逸度控制</td><td>氧逸度计：$\left(\frac{Ce^{4+}}{Ce^{3+}}\right)_{zircon}=\frac{Ce_{melt}-\frac{Ce_{zircon}}{D_{Ce^{3+}}^{zircon/melt}}}{\frac{Ce_{zircon}}{D_{Ce^{4+}}^{zircon/melt}}-Ce_{melt}}$
（Ce_{melt}是熔体中Ce含量，Ce_{zircon}是锆石Ce的含量；D是分配系数，是通过对3价稀土元素和4价元素（Zr、U、Th、Hf）线性拟合得到的）</td><td>适用条件：需要知道的先决条件较多，如母岩浆的主量成分，结晶温度和水含量；局限性：该氧逸度计对于母岩浆中的水含量特别敏感，水含量估算稍微有差别就会导致该方法估算的岩浆氧逸度差别很大</td><td>Ballard et al., 2002；Shu et al., 2019</td></tr>
</table>

续表 2

Continued Table 2

<table>
<tr><th colspan="2">分类</th><th>基本原理</th><th>氧逸度定性评估或定量计算方法</th><th>适用性</th><th>数据来源</th></tr>
<tr><td rowspan="2">多价元素矿物/熔体分配系数</td><td rowspan="2">锆石 Ce^{4+}/Ce^{3+} Ce_N/Ce_N^* Eu_N/Eu_N^*</td><td rowspan="2">多价元素（如Ce、Eu）在锆石/熔体之间的分配系数受氧逸度控制</td><td>利用Ce异常和锆石饱和温度计算氧逸度：
$\ln\left(\frac{Ce}{Ce^*}\right)_D=(0.1156\pm0.0050)\times\ln f(O_2)+\frac{13860\pm708}{T(K)}-6.125\pm0.484$
$\lg(Ti_{zir})=(5.711\pm0.072)-\frac{4800\pm86}{T(K)}-\lg\alpha_{SiO_2}+\lg\alpha_{TiO_2}$
（$\left(\frac{Ce}{Ce^*}\right)_D$指锆石的Ce分配系数异常，$T$为锆石结晶温度的绝对值，$\alpha_{SiO_2}$、$\alpha_{TiO_2}$为$SiO_2$、$TiO_2$的活度）</td><td>适用条件：适用于花岗质熔体中的锆石，能否应用到其他熔体成分还需要进一步研究；
局限性：单个锆石的La和Pr含量常常接近或者低于检出限，常常导致计算出来的氧逸度范围很大</td><td>Ferry et al.，2007；Trail et al.，2012；Dilles et al.，2015</td></tr>
<tr><td>Ce^{4+}/Ce^{3+}、Ce_N/Ce_N^*、Eu_N/Eu_N^*比值判断岩浆相对氧逸度</td><td>适用条件：需考虑锆石中混入的富含La的包裹体、斜长石结晶、岩浆在同化混染过程中可能混杂含斜长石的围岩等影响</td><td>Ballard et al.，2002；Trail et al.，2012；Zhou et al.，2018</td></tr>
<tr><td rowspan="4">矿物化学成分</td><td>锆石微量元素</td><td rowspan="4">矿物化学成分与氧逸度具有线性关系</td><td>$\lg f(O_2)_{sample}-\lg f(O_2)_{FMQ}=3.99_8(\pm0.12_4)\times\lg\left(\frac{Ce}{\sqrt{U_i\times Ti}}\right)+2.28_4(\pm0.10_1)$（$\lg f(O_2)_{sample}-\lg f(O_2)_{FMQ}$为样品氧逸度相对于QFM缓冲剂的值，也可以表达为ΔQFM，U_i为锆石结晶时U的含量)</td><td>适用条件：适用岩石类型范围很广，不需要单独测定结晶的温度、压力或者母熔体成分；氧逸度的适用范围为ΔQFM=−4.9~+2.9</td><td>Loucks et al.，2020</td></tr>
<tr><td>角闪石主量元素</td><td>ΔNNO=1.644Mg*−4.01
$Mg^*=Mg+\frac{Si}{47}-\frac{Al}{9}-1.3Ti+\frac{Fe^{3+}}{3.7}+\frac{Fe^{2+}}{5.2}-\frac{^{B}Ca}{20}-\frac{^{A}Na}{2.8}+\frac{^{A}[\,]}{9.5}$（$Al$、$Ti$分别表示六次配位的Al和Ti的原子数，$^{B}Ca$、$^{A}Na$、$^{A}[\,]$分别表示B组中的Ca、A组中的Na和A组中除Na、K外的剩余元素的原子数）</td><td>适用条件：适用于550~1120℃和＜1200MPa，−1≤ΔNNO≤+5的岩浆；
局限性：适用于钙碱性浅成-喷出岩</td><td>Ridolfi et al.，2008；2010</td></tr>
<tr><td rowspan="2">黑云母 Fe^{3+}-Fe^{2+}-Mg^{2+}图解、主量元素</td><td>Fe^{3+}-Fe^{2+}-Mg^{2+}图解法估算氧逸度</td><td>—</td><td>David et al.，1965</td></tr>
<tr><td>利用黑云母Ti温度作为与黑云母平衡的岩浆温度计算氧逸度
$t=\left\{\frac{\ln(Ti)-a-c(X_{Mg})^3}{b}\right\}^{0.333}$；$\lg f(O_2)=10.9-\frac{27000}{t}$
（温度t的单位为℃，Ti表示以22个氧原子为标准计算出的黑云母阳离子数中Ti的含量，X_{Mg}=Mg/(Mg+Fe)，$a=-2.3594$，$b=4.6482\times10^{-9}$，$c=-1.7283$）</td><td>适用条件：X_{Mg}=0.275~1.000，Ti=0.04~0.60，t=400~800℃为准确的校正范围</td><td>David et al.，1965；Henry et al.，2005</td></tr>
</table>

注：“—”表示适用范围较广，适用条件或局限性有待考证。

和成矿效应（Berry et al., 2009；Koleszar et al., 2009）。在斑岩成矿系统中，S、Cl等挥发性组分对Cu、Au等金属元素的运移和沉淀至关重要（Griffin et al.，2013；Tassara et al.，2017；Xu et al.，2021），主要表现为金属元素主要以S、Cl络合物的形式搬运，以金属硫化物的形式沉淀，如Cu、Au在熔体中低氧逸度条件下以氯络合物形式迁移，Au在高氧逸度条件下以硫氢络合物形式迁移，岩浆系统高氯含量有助于提高Cu、Au的溶解度（Zajacz et al.，2009）。因此，研究挥发分S、Cl等以及成矿元素本身的地球化学行为，有助于理解斑岩矿床成矿物质富集—演化过程（Richards，2015b）。

由于蚀变和风化作用，很难通过全岩研究岩浆挥发分。然而，磷灰石因其特殊的晶体结构，可接纳复杂微量元素的替换，富集了岩石圈地幔和地壳中普遍存在的挥发物（如Cl、S）和稀土元素等（O’Reil-

表 3 岩浆水含量常用测算方法

Table 3 Methods commonly used to estimate magmatic water content

分类	基本原理	测算方法	数据来源
地球化学特征与结晶分异作用估算水含量	岩浆中较高的 H_2O 含量(> 4%),在一定程度上抑制斜长石和钛铁矿的结晶分异,同时促进角闪石的结晶分异	全岩高 Sr/Y、La/Yb 和低 Y,高 Al_2O_3/TiO_2、V/Sc 等的特征,指示原始岩浆具有较高的含水量	Richards,2011;Loucks,2014;Wang et al.,2014
花岗岩地质湿度计(锆饱和温度计估算岩浆含水量)	对于 Zr 溶解度达到饱和的岩浆,Zr 含量主要受控于岩浆中温度和氧化性组分的变化,而对压力与水含量的变化不敏感	锆石饱和温度和富钾钙碱性英安岩结晶实验得出的水-温度平衡相图估算岩浆水含量	Naney,1983;Watson et al.,1983;Lu et al.,2015
高温高压熔融实验	埃达克岩成因研究,熔融实验的正演、反演方法	使用玄武质原岩熔融并将产物与天然板片熔体进行对比,判断岩浆形成需要的温度—压力(t-p)条件	Sen et al.,1994
		利用具有典型埃达克岩属性的 Pinatubo 英安岩开展高温高压熔融实验,揭示原始熔体的温度-压力-含水量(t-p-H_2O)	Prouteau et al.,2003
岩石学模拟	通过岩石学模型对岩浆形成与演化过程中组分与物理化学条件进行模拟计算	基于蒙特卡罗(Monte Carlo)法的岩石学和地球化学建模	Chiaradia et al.,2017;Chiaradia,2020
斜长石—流体湿度计	岩浆中斜长石的成分对温度和溶解水浓度非常敏感	基于斜长石—流体间的钙长石($CaAl_2Si_2O_8$)和钠长石($NaAlSi_3O_8$)置换反应建立的斜长石—流体湿度计(和温度计)估算水含量	Lange et al.,2009;Waters et al.,2015
角闪石主量元素	角闪石的化学成分与岩浆的结晶条件(温度、压力、氧逸度和含水量等)有关	$H_2O_{melt}=5.215Al^*+12.28$ $Al^*=Al+\frac{Al}{13.9}-\frac{Si+Ti}{5}-\frac{Fe^{2+}}{3}-\frac{Mg}{1.7}+\frac{^{B}Ca+{^{A}[\ ]}}{1.2}+\frac{^{A}Na}{2.7}-1.56K-\frac{Fe^{\#}}{1.6}$($Al$、$Ti$ 分别表示六次配位的 Al 和 Ti 的原子数,^{B}Ca、^{A}Na、$^{A}[\ ]$ 分别表示 B 组中的 Ca、A 组中的 Na 和 A 组中除 Na、K 外的剩余元素的原子数)	Ridolfi et al.,2008;2010
SIMS 锆石水含量测定	锆石封闭性好、易保存,其组分含量是反映原始岩浆成分特征的重要参数	基于二次离子质谱仪测定锆石氧同位素的同时测定锆石水含量	Xia et al.,2019;Cui et al.,2022

ly et al.,2000;Bruand et al.,2019),特别是磷灰石在斑岩系统中早期结晶(Mao et al.,2016)。因此,磷灰石可以更完整地记录这些岩浆中挥发分的演化历史(Chelle-Michou et al.,2017),其矿物结构和成分可以有效限定复杂岩浆热液成矿体系中的物理化学信息,从而有效约束斑岩成矿体系的复杂岩浆-热液过程(赵俊兴等,2021),而成为研究成岩成矿过程的理想"矿物探针"(Qu et al.,2021)。研究表明,在哈萨克斯坦地区斑岩 Cu 矿、西藏班公湖-怒江带俯冲期斑岩 Cu-Au 矿、冈底斯后碰撞环境斑岩 Cu-Mo 矿以及 Biga 半岛斑岩成矿带和 Afyon-Konya 成矿带等,这些俯冲、碰撞-后碰撞和伸展环境的斑岩矿床形成过程中,成矿期高氧逸度岩浆中的磷灰石常具有较高的 SO_3 含量(Cao et al.,2016;Tang et al.,2020;Li et al.,2021;赵俊兴等,2021;Cao et al.,2022a)。因此,可以根据磷灰石 SO_3 含量准确区分成矿斑岩与无矿岩体,而成为岩浆成矿潜力预测的有效指标。

6.5 岩浆混合作用

除富硫和金属的源区、较高的岩浆氧逸度、水含量以及 S、Cl 等挥发分外,钾质镁铁质岩浆注入引起的强烈岩浆混合作用也可能是形成超大型斑岩矿床的一个关键过程,因为该过程可能为斑岩系统提供部分金属(Au、Cu)、S、Cl 和 H_2O(Hou et al.,2013a)。这种现象在特提斯成矿域的土耳其西部(赵俊兴等,2021)、普朗(Cao et al.,2022b)、北衙(He et al.,2016)、马厂箐(Zhou et al.,2019;Shen et al.,2021)以及美国的 Bingham Canyon(Hattori et al.,2001)、菲律宾的 Baguio 矿集区(Cao et al.,2018)等斑岩系统中较为普遍。镁铁质的超钾质岩浆的水溶解度(~11.5%;500 MPa)比玄武岩(~9.5%;500 MPa)更高,并随压力的增大而增加(Behrens et al.,2009)。因此极度富水的幔源超钾质岩浆注入地壳底部诱发地壳熔融,或直接注入长英质岩浆房,为斑岩岩浆系统提供额外的水(Yang et al.,2015;Wang et al.,2016;Shen et al.,2021;Zheng et al.,2021)。

这一幔源超钾质岩浆水注入模式的关键证据有：① 马厂箐广泛发育于埃达克质岩浆中的镁铁质微粒包体（MME）中发现仅在同期超钾质岩中才含有的金云母，表明超钾质岩浆注入了埃达克质岩浆（Shen et al.，2021）；② 在冈底斯下地壳麻粒岩包体中发现富 F-Ti 金云母和高硅白云母，表明西藏下地壳曾被富水超钾质岩浆改造（Wang et al.，2016）；③ 在驱龙矿区发现与成矿斑岩时空相依的高镁闪长斑岩，暗示富水的超钾质岩浆曾与成矿岩浆混合（Yang et al.，2015）。镁铁质岩浆注入往往会形成近同时期侵位的镁铁质侵入体和镁铁质暗色包体（MME），这些镁铁质侵入体和暗色包体的成因、组分信息，可以示踪岩浆演化过程及对成矿的贡献，进而为研究深部岩浆储库演化过程及成矿控制因素提供依据。

7　研究展望

斑岩型矿床作为全球 Cu、Mo、Au、Re、Se、Te 等战略性矿产的主要来源（Sillitoe，2010；杨志明等，2020），蕴藏着巨大的经济价值，一直是国际矿业界的重点勘查目标和矿床学家们研究的热点课题。尽管俯冲有关的岩浆弧环境斑岩 Cu 矿成矿理论已日臻成熟（Sillitoe，2010），但仍尚存一些科学问题有待深刻揭示，如导致斑岩 Cu 矿超大规模产出的关键要素和有效过程（Richards，2013）、斑岩 Cu 矿岩浆演化的构造动力学背景、成矿金属 Cu 的富集过程与迁移机制（特别是金属 Cu 与 S 在成矿流体中的迁移机制）（Wilkinson，2013；Lee，2014；Blundy et al.，2015）等。近年来非弧环境斑岩矿床的研究是对斑岩 Cu 矿经典理论和传统认识的补充和完善，特别是与碰撞有关的斑岩 Cu 矿的研究已经取得了重要的阶段性成果（Hou et al.，2015b；2017）。但仍有几方面的问题需要深入，侯增谦等（2020a）将其概括为：① 下地壳生长过程与金属富集/亏损机制；② 浅部地壳精细结构对斑岩成矿系统的制约机制；③ 岩浆房详细过程与成矿物质迁移富集；④ 成矿环境对蚀变-矿化分带的控制机制。此外，大陆内部斑岩 Cu 矿，由于其时空分布与同时期俯冲带具有明显不协调的关系（李晓峰等，2019），其成因机制及其动力学过程还不十分清楚。这些有关斑岩矿床研究的国际前沿问题，也是矿床学研究的热点和难点。

不同地质构造背景（岛弧、陆缘弧、陆-陆碰撞、陆内环境）下，控制大型斑岩矿床形成的关键因素及其地球动力学机制一直是矿床学研究的重大科学问题。上述岩浆的源区、岩浆性质（氧逸度、含水量、挥发分等）、岩浆混合作用等方面的研究，能约束斑岩矿床成矿岩浆条件及其演变过程，为揭示斑岩矿床成矿机制提供重要信息。此外，还应该关注岩石圈属性与结构、地壳厚度与深部结构、岩石圈构造变形与大型矿集区形成就位机制、岩浆房大小、岩浆侵位深度、岩浆热液活动历史及其冷却速率以及成矿物质来源等。这些问题的深入对于完善斑岩成矿系统的成矿理论及指导相关找矿勘查具有重要科学意义。

致　谢　论文撰写过程中参考了大量前人资料，但限于作者学识，所作的论述不够透彻、详尽，谨此表示谢忱和歉意。王乐博士审阅初稿，提出重要的修改建议；审稿专家对本文提出宝贵修改意见。在此一并致以诚挚的谢意！

References

Aghazadeh M, Hou Z Q, Badrzadeh Z and Zhou L M. 2015. Temporal-spatial distribution and tectonic setting of porphyry copper deposits in Iran: Constraints from zircon U-Pb and molybdenite Re-Os geochronology[J]. Ore Geology Reviews, 70: 385-406.

Audétat A, Pettke T and Dolejš D. 2004. Magmatic anhydrite and calcite in the ore-forming quartz-monzodiorite magma at Santa Rita, New Mexico (USA): Genetic constraints on porphyry-Cu mineralization[J]. Lithos, 72(3-4): 147-161.

Ballard J R, Palin M J and Campbell I H. 2002. Relative oxidation states of magmas inferred from Ce(Ⅳ)/Ce(Ⅲ) in zircon: Application to porphyry copper deposits of northern Chile[J]. Contributions to Mineralogy and Petrology, 144(3): 347-364.

Behrens H, Misiti V, Freda C, Vetere F, Botcharnikov R E and Scarlato P. 2009. Solubility of H_2O and CO_2 in ultrapotassic melts at 1200 and 1250°C and pressure from 50 to 500 MPa[J]. American Mineralogist, 94(1): 105-120.

Berry A J, Harris A C, Kamenetsky V S, Newvile M and Sutton S R. 2009. The speciation of copper in natural fluid inclusions at temperatures up to 700℃[J]. Chemical Geology, 259(1-2): 2-7.

Bi X W, Hu R Z, Pen J T, Wu K X, Su W C and Zhan X Z. 2005. Geochemical characteristics of the Yao'an and Machangqing alkaline-rich intrusions[J]. Acta Petrologica Sinica, 21(1): 113-124(in Chinese with English abstract).

Blundy J, Mavrogenes J, Tattitch B, Sparks S and Gilmer A. 2015. Generation of porphyry copper deposits by gas-brine reaction in volcanic arcs[J]. Nature Geoscience, 8(3): 235-240.

Braxton D P, Cooke D R, Dunlap J, Norman M, Reiners P, Stein H and Waters P. 2012. From crucible to graben in 2.3 Ma: A highresolution geochronological study of porphyry life cycles, Boyongan-Bayugo copper-gold deposits, Philippines[J]. Geology, 40(5): 471-474.

Bruand E, Storey C, Fowler M and Heilimo E. 2019. Oxygen isotopes in titanite and apatite, and their potential for crustal evolution research[J]. Geochimica et Cosmochimica Acta, 255: 144-162.

Buddington A F and Lindsley D H. 1964. Iron-titanium oxide minerals and synthetic equivalents[J]. Journal of Petrology, 5(2): 310-357.

Cai K D, Sun M, Yuan C, Zhao G C, Xiao W J, Long X P and Wu F Y. 2011. Geochronology, petrogenesis and tectonic significance of peraluminous granites from the Chinese Altai, NW China[J]. Lithos, 127(1-2): 261-281.

Cameron E M. 1989. Scouring of gold from the lower crust[J]. Geology, 17(1): 26-29.

Candela P A and Piccoli P M. 2005. Magmatic processes in the development of porphyry-type ore systems[M]. Society of Economic Geologists, Special Publication. 25-37.

Canil D. 2002. Vanadium in peridotites, mantle redox and tectonic environments: Archean to present[J]. Earth and Planetary Science Letters, 195(1-2): 75-90.

Cao K, Yang Z M, Hou Z Q, White N C and Yu C. 2022a. Contrasting porphyry Cu fertilities in the Yidun arc, eastern Tibet: Insights from zircon and apatite compositions and implications for exploration[M]. Society of Economic Geologists, Special Publication. 24 (2): 231-255.

Cao K, Yang Z M, White N C and Hou Z Q. 2022b. Generation of the giant porphyry Cu-Au deposit by repeated recharge of mafic magmas at Pulang in eastern Tibet[J]. Econ. Geol., 117(1): 57-90.

Cao M J, Li G M, Qin K Z, Evans N J and Seitmuratova E Y. 2016. Assessing the magmatic affinity and petrogenesis of granitoids at the giant Aktogai porphyry Cu deposit, Central Kazakhstan[J]. American Journal of Science, 316(7): 614-668.

Cao M J, Evans N J, Hollings P, Cooke D R, McInnes B I A, Qin K Z and Li G M. 2018. Phenocryst zonation in porphyry-related rocks of the Baguio district, Philippines: Evidence for magmatic and metallogenic processes[J]. Journal of Petrology, 59(5): 825-848.

Chelle-Michou C and Chiaradia M. 2017. Amphibole and apatite insights into the evolution and mass balance of Cl and S in magmas associated with porphyry copper deposits[J]. Contributions to Mineralogy and Petrology, 172(105): 1-26.

Chen B, Jahn B M, Arakawa Y and Zhai M G. 2004. Petrogenesis of the Mesozoic intrusive complexes from the southern Taihang Orogen, North China Craton: Elemental and Sr-Nd-Pb isotopic constraints[J]. Contributions to Mineralogy and Petrology, 148(4): 489-501.

Chen B, Tian W, Jahn B M and Chen Z C. 2008. Zircon SHRIMP U-Pb ages and in-situ Hf isotopic analysis for the Mesozoic intrusions in South Taihang, North China Craton: Evidence for hybridization between mantle-derived magmas and crustal components[J]. Lithos, 102(1-2): 118-137.

Chen H Y and Wu C. 2020. Metallogenesis and major challenges of porphyry copper systems above subduction zones[J]. Science China Earth Sciences, 63(7):899-918.

Chen J L, Xu J F, Ren J B, Huang X X and Wang B D. 2014. Geochronology and geochemical characteristics of Late Triassic porphyritic rocks from the Zhongdian arc, eastern Tibet, and their tectonic and metallogenic implications[J]. Gondwana Research, 26(2): 492-504.

Chen J L, Xu J F, Ren J B and Huang X X. 2017. Late Triassic E-MORB-like basalts associated with porphyry Cu-deposits in the southern Yidun continental arc, eastern Tibet: Evidence of slab-tear during subduction[J]? Ore Geology Reviews, 90:1054-1062.

Chen Y J, Zhai M G and Jiang S Y. 2009. Significant achievements and open issues in study of orogenesis and metallogenesis surrounding the North China continent[J]. Acta Petrologica Sinica, 25 (11): 2695-2726(in Chinese with English abstract).

Chen Y J, Zhang C, Wang P, Pirajno F and Li N. 2017. The Mo deposits of Northeast China: A powerful indicator of tectonic settings and associated evolutionary trends[J]. Ore Geology Reviews, 81 (2): 602-640.

Chiaradia M and Caricchi L. 2017. Stochastic modelling of deep magmatic controls on porphyry copper deposit endowment[J]. Scientific Reports, 7: 1-11.

Chiaradia M. 2020. How much water in basaltic melts parental to porphyry copper deposits[J]? Frontiers in Earth Science, 8: 138.

Chung S L, Chu M F, Zhang Y Q, Xie Y W, Lo C H, Lee T Y, Lan C Y, Li X H, Zhang Q and Wang Y Z. 2005. Tibetan tectonic evolution inferred from spatial and temporal variations in post-collisional magmatism[J]. Earth-Science Reviews, 68(3-4): 173-196.

Ciobanu C L, Cook N J and Stein H. 2002. Regional setting and geochronology of the Late Cretaceous banatitic magmatic and metallogenetic belt[J]. Mineralium Deposita, 37(6-7): 541-567.

Cline J S and Bodnar R J. 1991. Can economic porphyry copper mineralization be generated by a typical calc-alkaline melt[J]? Journal of Geophysical Research: Solid Earth, 96(B5): 8113-8126.

Cooke D R, Hollings P and Walsh J L. 2005. Giant porphyry deposits: Characteristics, distribution, and tectonic controls[J]. Econ. Geol., 100(5): 801-818.

Cooke D R, Hollings P, Wilkinson J J and Tosdal R M. 2014. Treatise on geochemistry[A]. Geochemistry of porphyry deposits[C]. 2nd ed. Elsevier, Oxford, 13: 357-381.

Cox D, Watt S F L, Jenner F E, Hastie A R, Hammond S J and Kunz B E. 2020. Elevated magma fluxes deliver high-Cu magmas to the upper crust[J]. Geology, 48(10): 957-960.

Cui Z X, Xia X P, Yang Q, Gong B, Zhang W F, Zhang Y Q and Lai C K. 2022. SIMS zircon hydrogen isotope and H_2O content analyses and reference material development[J]. Journal of Analytical Atomic Spectrometry, 43(1): 70-76.

David R W and Hans P E. 1965. Stability of biotite: Experiment, theory, and application[J]. American Mineralogist, 50(9): 1228-1272.

Deng J, Hou Z Q, Mo X X, Yang L Q, Wang Q F and Wang C M. 2010. Superimposed orogenesis and metallogenesis in Sanjiang Tethys[J]. Mineral Deposits, 29(1): 37-42(in Chinese with English abstract).

Deng J, Wang Q F, Li G J and Santosh M. 2014. Cenozoic tectono-magmatic and metallogenic processes in the Sanjiang region, southwestern China[J]. Earth-Science Reviews, 138(1): 268-299.

Deng J, Wang Q F, Li G J, Hou Z Q, Jiang C Z and Danyushevsky L. 2015. Geology and genesis of the giant Beiya porphyry-skarn gold deposit, northwestern Yangtze Block, China[J]. Ore Geology Reviews, 70: 457-485.

Deng J, Wang Q F, Gao L, He W Y, Yang Z Y, Zhang S H, Chang L J, Li G J, Sun X and Zhou D Q. 2021. Differential crustal rotation and its control on giant ore clusters along the eastern margin of Tibet[J]. Geology, 49(4): 428-432.

Dilles J H, Kent A J R, Wooden J L, Tosdal R M, Koleszar A, Lee R G and Farmer L P. 2015. Zircon compositional evidence for sulfur-degassing from ore-forming magmas[J]. Econ. Geol., 110(1):241-251.

Ding L, Maksatbek S, Cai F L, Wang H Q, Song P P, Ji W Q, Xu Q, Zhang L Y, Muhammad Q and Upendra B. 2017. Processes of initial collision and suturing between India and Asia[J]. Science China Earth Sciences, 60(4): 635-651.

Fan Y, Zhou T F, Zhang D Y, Yuan F, Fan Y, Ren Z and White N C. 2014. Spatial and temporal distribution and metallogical background of the Chinese molybdenum deposits[J]. Acta Geologica Sinica, 88(4): 784-804(in Chinese with English abstract).

Ferry J M and Watson E B. 2007. New thermodynamic models and revised calibrations for the Ti-in-zircon and Zr-in-rutile thermometers[J]. Contributions to Mineralogy and Petrology, 154(4): 429-437.

Gao J, Klemd R, Zhu M T, Wang X S, Li J L, Wan B, Xiao W J, Zeng Q D, Shen P, Sun J G, Qin K Z and Campos E. 2018. Large-scale porphyry-type mineralization in the Central Asian metallogenic domain: A review[J]. Journal of Asian Earth Sciences, 165: 7-36.

Gao J, Zhu M T, Wang X S, Hong T, Li G M, Li J L, Xiao W J, Qin K Z, Zeng Q D, Shen P, Xu X W, Zhang Z C, Zhou J B, Lai Y, Zhang X H, Sun J G and Wang B. 2019. Large-scale porphyry-type mineralization in the Central Asian metallogenic domain: Tectonic background, fluid feature and metallogenic deep dynamic mechanism[J]. Acta Geologica Sinica, 93(1): 24-71(in Chinese with English abstract).

Gao Y F, Hou Z Q, Kamber B S, Wei R H, Meng X J and Zhao R S. 2007. Adakite-like porphyries from the southern Tibetan continental collision zones: Evidence for slab melt metasomatism[J]. Contributions to Mineralogy and Petrology, 153(1): 105-120.

Gao Y F, Yang Z S, Santosh M, Hou Z Q, Wei R H and Tian S H. 2010. Adakitic rocks from slab melt-modified mantle sources in the continental collision zone of southern Tibet[J]. Lithos, 119(3-4): 651-663.

Gao Y F, Santosh M, Wei R H, Ma G X, Chen Z K and Wu J L. 2013. Origin of high Sr/Y magmas from the northern Taihang Mountains: Implications for Mesozoic porphyry copper mineralization in the North China Craton[J]. Journal of Asian Earth Sciences, 78: 143-159.

Geng Q R, Pan G T, Wang L Q, Peng Z M and Zhang Z. 2011. Tethyan evolution and metallogenic geological background of the Bangong Co-Nujiang belt and the Qiangtang massif in Tibet[J]. Geological Bulletin of China, 30(8): 1261-1274(in Chinese with English abstract).

Ghiorso M S and Evans B W. 2008. Thermodynamics of rhombohedral oxide solid solutions and a revision of the FE-TI two-oxide geothermometer and oxygen-barometer[J]. American Journal of Science, 308(9): 957-1039.

Griffin W L, Begg G C and O'Reilly S Y. 2013. Continental-root control on the genesis of magmatic ore deposits[J]. Nature Geoscience, 6(11): 905-910.

Guo Z F, Wilson M and Liu J Q. 2007. Post-collisional adakites in South Tibet: Products of partial melting of subduction-modified lower crust[J]. Lithos, 96(1-2): 205-224.

Gustafson L B and Hunt J P. 1975. The porphyry copper deposit at El Salvador, Chile[J]. Econ. Geol., 70(5): 857-912.

Harrison R L, Maryono A, Norris M S, Rohrlach B D, Cooke D R, Thompson J M, Creaser R A and Thiede D S. 2018. Geochronology of the Tumpangpitu porphyry Au-Cu-Mo and high-sulfidation epithermal Au-Ag-Cu deposit: Evidence for pre- and postmineralization diatremes in the Tujuh Bukit district, Southeast Java, Indonesia[J]. Econ. Geol., 113(1): 163-192.

Hattori K H and Keith J D. 2001. Contribution of mafic melt to porphyry copper mineralization: Evidence from Mount Pinatubo, Philippines, and Bingham Canyon, Utah, USA[J]. Mineralium Deposita, 36(8): 799-806.

He W Y, Mo X X, Yang L Q, Xing Y L, Dong G C, Yang Z, Gao X and Bao X S. 2016. Origin of the Eocene porphyries and mafic microgranular enclaves from the Beiya porphyry Au polymetallic deposit, western Yunnan, China: Implications for magma mixing/mingling and mineralization[J]. Gondwana Research, 40: 230-248.

Henry D J, Guidotti C V and Thomson J A. 2005. The Ti-saturation surface for low-to-medium pressure metapelitic biotites: Implications for geothermometry and Ti-substitution mechanisms[J]. American Mineralogist, 90(2-3): 316-328.

Hou T, Botcharnikov R, Moulas E, Just T, Berndt J, Koepke J, Zhang Z C, Wang M, Yang Z P and Holtz F. 2021. Kinetics of Fe-Ti oxide re-equilibration in magmatic systems: Implications for thermo-oxybarometry[J]. Journal of Petrology, 61(11-12): 1-24.

Hou Z Q, Wang L Q, Zaw K, Mo X X, Wang M J, Li D M and Pan G T. 2003a. Post-collisional crustal extension setting and VHMS mineralization in the Jinshajiang orogenic belt, southwestern China[J]. Ore Geology Reviews, 22(3-4): 177-199.

Hou Z Q, Ma H W, Zaw K, Zhang Y Q, Wang M J, Wang Z, Pan G T and Tang R L. 2003b. The Himalayan Yulong porphyry copper belt: product of large-scale strike-slip faulting in eastern Tibet[J]. Econ. Geol., 98(1): 125-145.

Hou Z Q, Gao Y F, Qu X M, Rui Z Y and Mo X X. 2004. Origin of adakitic intrusives generated during Mid-Miocene East-West extension in southern Tibet[J]. Earth and Planetary Science Letters, 220(1-2): 139-155.

Hou Z Q, Gao Y F, Meng X J, Qu X M and Huang W. 2004a. Genesis of adakitic porphyry and tectonic controls on the Gangdese Miocene porphyry copper belt in the Tibetan orogen[J]. Acta Petrologica Sinica, 20(2): 239-248(in Chinese with English abstract).

Hou Z Q, Yang Y Q, Qu X M, Huang D H, Lü Q T, Wang H P, Yu J J and Tang S H. 2004b. Tectonic evolution and mineralization systems of the Yidun arc orogen in Sanjiang region, China[J]. Acta Geologica Sinica, 78(1): 109-120(in Chinese with English abstract).

Hou Z Q, Mo X X, Yang Z M, Wang A J, Pan G T, Qu X M and Nie F J. 2006a. Metallogeneses in the collisional orogen of the Qinghai-Tibet Plateau：Tectonic setting, tempo-spatial distribution and ore deposit types[J]. Geology in China, 33(2): 340-351(in Chinese with English abstract).

Hou Z Q, Yang Z S, Xu W Y, Mo X X, Ding L, Gao Y F, Dong F L, Li G M, Qu X M, Li G M, Zhao Z D, Jiang S H, Meng X J, Li Z Q, Qin K Z and Yang Z M. 2006b. Metallogenesis in Tibetan collisional orogenic belt: I. Mineralization in main collisional orogenic setting[J]. Mineral Deposits, 25(4): 337-358(in Chinese with English abstract).

Hou Z Q, Pan X F, Yang Z M and Qu X M. 2007. Porphyry Cu-(Mo-Au) deposits no related to oceanic-slab subduction: Examples from Chinese porphyry deposits in continental settings[J]. Geoscience, 21(2): 332-351(in Chinese with English abstract).

Hou Z Q, Yang Z M, Qu X M, Meng X J, Li Z Q, Beaudoin G, Rui Z Y, Gao Y F and Zaw K. 2009. The Miocene Gangdese porphyry copper belt generated during post-collisional extension in the Tibetan orogeny[J]. Ore Geology Reviews, 36(1-3): 25-51.

Hou Z Q and Yang Z M. 2009. Porphyry deposits in continental settings of China: Geological characteristics, magmatic-hydrothermal system, and metallogenic model[J]. Acta Geologica Sinica, 83 (12): 1779-1817(in Chinese with English abstract).

Hou Z Q, Zhang H R, Pan X F and Yang Z M. 2011. Porphyry Cu (-Mo-Au) deposits related to melting of thickened mafic lower crust: Examples from the eastern Tethyan metallogenic domain[J]. Ore Geology Reviews, 39(1-2): 21-45.

Hou Z Q, Zheng Y C, Yang Z M, Rui Z Y, Zhao Z D, Jiang S H, Qu X M and Sun Q Z. 2013a. Contribution of mantle components within juvenile lower-crust to collisional zone porphyry Cu systems in Tibet[J]. Mineralium Deposita, 48(2): 173-192.

Hou Z Q, Pan X F, Li Q Y, Yang Z M and Song Y C. 2013b. The giant Dexing porphyry Cu-Mo-Au deposit in East China: Product of melting of juvenile lower crust in an intracontinental setting[J]. Mineralium Deposita, 48(8): 1019-1045.

Hou Z Q and Zhang H R. 2015a. Geodynamics and metallogeny of the eastern Tethyan metallogenic domain[J]. Ore Geology Reviews, 70: 346-384.

Hou Z Q, Yang Z M, Lu Y J, Kemp A, Zheng Y C, Li Q Y, Tang J X, Yang Z S and Duan L F. 2015b. A genetic linkage between subduction- and collision-related porphyry Cu deposit in continental collision zone[J]. Geology, 42(3): 247-250.

Hou Z Q, Duan L F, Lu Y J, Zheng Y C, Zhu D C, Yang Z M, Yang Z S, Wang B D, Pei Y R, Zhao Z D and McCuaig T C. 2015c. Lithospheric architecture of the Lhasa terrane and its control on ore deposits in the Himalayan-Tibetan orogen[J]. Econ. Geol., 110(6): 1541-1575.

Hou Z Q, Li Z Q, Gao Y F, Lu Y J, Yang Z M, Wang R and Shen Z C. 2015d. Lower-crustal magmatic hornblendite in North China Craton Insight into the genesis of porphyry Cu deposits[J]. Econ. Geol., 110(7): 1879-1904.

Hou Z Q, Zhou Y, Wang R, Zheng Y C, He W Y, Zhao M, Evans N J and Weinberg R F. 2017. Recycling of metal-fertilized lower continental crust: Origin of non-arc Au-rich porphyry deposits at cratonic edges[J]. Geology, 45(6): 563-566.

Hou Z Q and Wang T. 2018. Isotopic mapping and deep material probing (Ⅱ): Imaging crustal architecture and its control on mineral systems[J]. Earth Science Frontiers, 25(6): 20-41(in Chinese with English abstract).

Hou Z Q and Wang R. 2019. Fingerprinting metal transfer from mantle[J]. Nature Communications, 10: 1-3.

Hou Z Q, Yang Z M, Wang R and Zheng Y C. 2020a. Further discussion on porphyry Cu-Mo-Au deposit formation in Chinese mainland[J]. Earth Science Frontiers, 27(2): 20-44(in Chinese with English abstract).

Hou Z Q, Zheng Y C, Lu Z W, Xu B, Wang C M and Zhang H R. 2020b. Growth, thickening and evolution of the thickened crust of the Tibet Plateau[J]. Acta Geologica Sinica, 94(10): 2797-2815(in Chinese with English abstract).

Htut T Y, Qin K Z, Li G M, Sein K and Evans N J. 2020. Eocene arc magmatism and related Cu-Au (Mo) mineralization in the Shangalon-Kyungalon district, Wuntho-Popa Arc, northern Myanmar[J]. Ore Geology Reviews, 125:103678.

Hu R Z, Mao J W, Hua R M and Fan W M. 2015. Intra-continental mineralization of South China Craton[M]. Beijing: Science Press. 1-903(in Chinese).

Hu X M, Wang J G, An W, Garzanti E and Li J. 2017. Constraining the timing of the India-Asia continental collision by the sedimentary record[J]. Science China Earth Sciences, 60(4):603-625.

Huang F, Wang D H, Wang C H, Chen Z H, Yuan Z X and Liu X X. 2014. Resources characteristics of molybdenum deposits and their regional metallogeny in China[J]. Acta Geologica Sinica, 88(12): 2296-2314(in Chinese with English abstract).

James D E and Sacks I S. 1999. Cenozoic formation of the Central Andes: A geophysical perspective[A]. In: Skinner B J, ed. Geology and ore deposits of the Central Andes[C]. Society of Economic Geologists, Special Publication, 7: 1-25.

Jiang Y H, Jiang S Y, Ling H F and Dai B Z. 2006. Low-degree melting of a metasomatized lithospheric mantle for the origin of Cenozoic Yulong monzogranite-porphyry, East Tibet: Geochemical and Sr-Nd-Pb-Hf isotopic constraints[J]. Earth and Planetary Science Letters, 241(3-4): 617-633.

Jugo P J, Luth R W and Richards J P. 2005. Experimental data on the speciation of sulfur as a function of oxygen fugacity in basaltic melts[J]. Geochimica et Cosmochimica Acta, 69(2): 497-503.

Jugo P J. 2009. Sulfur content at sulfide saturation in oxidized magmas[J]. Geology, 37(5): 415-418.

Kay S M and Mpodozis C. 2001. Central andean ore deposits linked to evolving shallow subduction systems and thickening crust[J]. Geological Society of America Today, 11(3): 4-9.

Kemp A I S, Hawkesworth C J, Paterson B A and Kinny P D. 2006. Episodic growth of the Gondwana supercontinent from hafnium and oxygen isotopes in zircon[J]. Nature, 7076(439): 580-583.

Kerrich R, Goldfarb R, Groves D I and Garwin S. 2000. The geodynamics of world-class gold deposits: Characteristics, space-time distribution and origins[M]. Society of Economic Geologists, Special Publication. 13: 501-551.

Klemm L M, Pettke T, Heinrich C A and Campos E. 2007. Hydrothermal evolution of the El Teniente deposit, Chile: Porphyry Cu-Mo ore deposition from low-salinity magmatic fluids[J]. Econ. Geol., 102(6): 1021-1045.

Koleszar A M, Saal A E, Hauri E H, Nagle A N, Liang Y and Kurz M D. 2009. The volatile contents of the Galapagos plume: Evidence for H_2O and F open system behavior in melt inclusions[J]. Earth and Planetary Science Letters, 287(3-4): 442-452.

Konecke B A, Fiege A, Simon A C, Parat F and Stechern A. 2017. Covariability of S^{6+}, S^{4+}, and S^{2-} in apatite as a function of oxidationstate: Implications for a new oxybarometer[J]. American Mineralogist, 102(3): 548-557.

Kress V C and Carmichael I S E. 1991. The compressibility of silicate liquids containing Fe_2O_3 and the effect of composition, temperature, oxygen fugacity and pressure on their redox states[J]. Contributions to Mineralogy and Petrology, 108(1-2): 82-92.

Kusky T, Li J H and Santosh M. 2007. The Paleoproterozoic North Hebei Orogen: North China Craton's collisional suture with the Columbia supercontinent[J]. Gondwana Research, 12(1-2): 4-28.

Lang X H, Tang J X, Li Z J, Huang Y, Ding F, Yang H H, Xie F W, Zhang L, Wang Q and Zhou Y. 2014. U-Pb and Re-Os geochronological evidence for the Jurassic porphyry metallogenic event of the Xiongcun district in the Gangdese porphyry copper belt, southern Tibet, PRC[J]. Journal of Asian Earth Sciences, 79: 608-622.

Lange R A, Frey H M and Hector J. 2009. A thermodynamic model for the plagioclase-liquid hygrometer/thermometer[J]. American Mineralogist, 94(4): 494-506.

Lanzirotti A, Dyar M D, Sutton S, Newville M, Head E, Carey C J, McCanta M, Lee L, King P L and Jones J. 2018. Accurate predictions of microscale oxygen barometry in basaltic glasses using V K-edge X-ray absorption spectroscopy: A multivariate approach[J]. American Mineralogist, 103(8): 1282-1297.

Lee C T A, Luffi P, Chin E J, Bouchet R, Dasgupta R, Morton D M, Le Roux V, Yin Q Z and Jin D. 2012. Copper systematics in arc magmas and implications for crust-mantle differentiation[J]. Science, 336(6077): 64-68.

Lee C T A. 2014. Economic geology: Copper conundrums[J]. Nature Geoscience, 7(1): 10-11.

Leng C B, Zhang X C, Zhong H, Hu R Z, Zhou W D and Li C. 2013. Re-Os molybdenite ages and zircon Hf isotopes of the Gangjiang porphyry Cu-Mo deposit in the Tibetan Orogen[J]. Mineralium Deposita, 48(5): 585-602.

Leng C B, Chen X L, Zhang J J, Ma X H, Tian F, Guo J H and Zhang L J. 2020. Lithogeochemical and mineral chemical footprints of porphyry Cu±Mo±Au deposits: A review[J]. Acta Geologica Sinica, 94(11): 3189-3212(in Chinese with English abstract).

Li C H, Shen P and Pan H D. 2018. Mineralogy of the Aktogai giant porphyry Cu deposit in Kazakhstan: Insights into the fluid composition and oxygen fugacity evolution[J]. Ore Geology Reviews, 95: 899-916.

Li C Y, Wang F Y, Hao X L, Ding X, Zhang H, Ling M X, Zhou J B, Li Y L, Fan W M and Sun W D. 2012. Formation of the world's largest molybdenum metallogenic belt: A plate-tectonic perspective on the Qinling molybdenum deposits[J]. International Geology Review, 54(9): 1093-1112.

Li J X, Qin K Z, Li G M, Richards J P, Zhao J X and Cao M J. 2014. Geochronology, geochemistry, and zircon Hf isotopic compositions of Mesozoic intermediate felsic intrusions in Central Tibet: Petrogenetic and tectonic implications[J]. Lithos, 198-199: 77-91.

Li J X, Zhang LY, Fan W M, Ding L, Sun Y L, Peng T P, Li G M and Sein K. 2018. Mesozoic-Cenozoic tectonic evolution and metallogeny in Myanmar: Evidence from zircon/cassiterite U-Pb and molybdenite Re-Os geochronology[J]. Ore Geology Reviews, 102: 829-845.

Li J X, Li G M, Evans N J, Zhao J X, Qin K Z and Xie J. 2021. Primary fluid exsolution in porphyry copper systems: Evidence from magmatic apatite and anhydrite inclusions in zircon[J]. Mineralium Deposita,56(2): 407-415.

Li W C, Yin G H, Lu Y X, Wang Y B, Yu H J, Cao X M and Zhang S Q. 2010. Delineation of Hongshan-Shudu ophiolite mélange in Geza volcanic-magmatic arc and its significance, Southwest “Jinsha-Lancang-Nu rivers”[J]. Acta Petrologica Sinica, 26(6): 1661-1671(in Chinese with English abstract).

Li W C, Xue Y X, Lu Y X, Xue S R and Ren Z J. 2014. The metallogical regularity and guidance for mineral exploration of porphyry-type copper deposits in China[M]. Beijing: Geological Publishing House. 1-411(in Chinese).

Li X F, Hua R M, Ma D S, Xu J, Qi Y Q, Wu L Y and Zhu Y T. 2019. Mesozoic sub-continental lithospheric mantle extension and related porphyry copper mineralization in South China[J]. Acta Petrologica Sinica, 35(1): 76-88(in Chinese with English abstract).

Li Y, Selby D, Condon D and Tapster S. 2017. Cyclic magmatic-hydrothermal evolution in porphyry systems: High-precision U-Pb and Re-Os geochronology constraints on the Tibetan Qulong porphyry Cu-Mo deposit[J]. Econ. Geol., 112(6): 1419-1440.

Li Z X A and Lee C T A. 2004. The constancy of upper mantle fO_2 through time inferred from V/Sc ratios in basalts[J]. Earth and Planetary Science Letters, 228(3-4): 483-493.

Liang H Y, Mo J H, Sun W D, Zhang Y Q, Zeng T, Hu G Q and Charllote M A. 2009. Study on geochemical composition and isotope ages of the Malasongduo porphyry associated with Cu-Mo mineralization[J]. Acta Petrologica Sinica, 25(2): 385-392(in Chinese with English abstract).

Ling M X, Wang F Y, Ding X, Hu Y H, Zhou J B, Zartman R E, Yang X Y and Sun W D. 2009. Cretaceous ridge subduction along the Lower Yangtze River Belt, eastern China[J]. Econ. Geol., 104(2): 303-321.

Liu Z, Tian X B, Yuan X H, Liang X F, Chen Y, Zhu G H, Zhang H S, Li W, Tan P, Zuo S C, Wu C L, Nie S T, Wang G C, Yu G P and Zhou B B. 2020. Complex structure of upper mantle beneath the Yadong-Gulu rift in Tibet revealed by S-to-P converted waves[J]. Earth and Planetary Science Letters, 531: 115954.

Loucks R R. 2014. Distinctive composition of copper-ore-forming arcmagmas[J]. Australian Journal of Earth Sciences, 61(1): 5-16.

Loucks R R, Fiorentini M L and Henríquez G J. 2020. New magmatic oxybarometer using trace elements in zircon[J]. Journal of Petrology, 61(3):1-30.

Lowell J D and Guilbert J M. 1970. Lateral and vertical alteration-mineralization zoning in porphyry ore deposits[J]. Econ. Geol., 65 (4): 373-408.

Lu Y J, Kerrich R, Kemp A I S, McCuaig T C, Hou Z Q, Hart C J R, Li Z X, Cawood P A, Bagas L, Yang Z M, Cliff J, Belousova E A, Jourdan F and Evans N J. 2013. Intracontinental Eocene-Oligocene porphyry Cu mineral systems of Yunnan, western Yangtze Craton, China: Compositional characteristics, sources, and implications for continental collision metallogeny[J]. Econ. Geol., 108 (7): 1541-1576.

Lu Y J, Loucks R R, Fiorentini M L, Yang Z M and Hou Z Q. 2015. Fluid flux melting generated postcollisional high Sr/Y copper oreforming water-rich magmas in Tibet[J]. Geology, 43(7): 583-586.

Luo C H, Wang R, Weinberg R F and Hou Z Q. 2022. Isotopic spatialtemporal evolution of magmatic rocks in the Gangdese belt: Implications for the origin of Miocene post-collisional giant porphyry deposits in southern Tibet[J]. Geological Society of America Bulletin, 134(1-2): 316-324.

Mao J W, Luo M C, Xie G Q, Liu J and Wu S H. 2014. Basic characteristics and new advances in research and exploration on porphyry copper deposits[J]. Acta Geologica Sinica, 88(12): 2153-2175(in Chinese with English abstract).

Mao M, Rukhlov A S, Rowins S M, Spence J and Coogan L A. 2016. Apatite trace element compositions: A robust new tool for mineral exploration[J]. Econ. Geol., 111(5): 1187-1222.

Maryono A, Harrison R L, Cooke D R, Rompo I and Hoschke T G. 2018. Tectonics and geology of porphyry Cu-Au deposits along the Eastern Sunda magmatic arc, Indonesia[J]. Econ. Geol., 113 (1): 7-38.

McInnes B I A, McBride J S, Evans N J, Lambert D D and Andrew A S. 1999. Osmium isotope constraints on ore metal recycling in subduction zones[J]. Science, 286(5439): 512-516.

Miles A, Graham C, Hawkesworth C, Gillespie M, Hinton R and Bromiley G. 2016. Reply to comment by Marks et al. (2016) on "Apatite: A new redox proxy for silicic magmas?" [Geochimica et Cosmochimica Acta 132 (2014) 101-119] [J]. Geochimica et Cosmochimica Acta, 183(1): 271-273.

Mo X X, Zhao Z D, Deng J F, Dong G C, Zhou S, Guo T Y, Zhang S Q and Wang L L. 2003. Response of volcanism to the India-Asia collision[J]. Earth Science Frontiers, 10(3): 135-148(in Chinese with English abstract).

Naney M T. 1983. Phase equilibria of rock-forming ferromagnesian silicates in granitic systems[J]. American Journal of Science, 283 (10): 993-1033.

O'Reilly S Y and Griffin W L. 2000. Apatite in the mantle: Implications for metasomatic processes and high heat production in Phanerozoic mantle[J]. Lithos, 53(3-4): 217-232.

Pan F B, Zhang H F, Harris N, Xu W C and Guo L. 2012. Oligocene magmatism in the eastern margin of the East Himalayan syntaxis and its implication for the India-Asia post-collisional process[J]. Lithos, 154: 182-192.

Peacock S M, Rushmer T and Thompson A B. 1994. Partial melting of subducting oceanic crust[J]. Earth and Planetary Science Letters, 121(1-2): 227-244.

Perelló J, Razique A, Schloderer J and Asad-ur-Rehman J. 2008. The Chagai porphyry copper belt, Baluchistan Province, Pakistan[J]. Econ. Geol., 103(8): 1583-1612.

Pettke T, Oberli F and Heinrich C A. 2010. The magma and metal source of giant porphyry-type ore deposits, based on lead isotope microanalysis of individual fluid inclusions[J]. Earth and Planetary Science Letters, 296(3-4): 267-277.

Prouteau G and Scaillet B. 2003. Experimental constraints on the origin of the 1991 Pinatubo dacite[J]. Journal of Petrology, 44 (12): 2203-2241.

Qin K Z, Li G M, Zhao J X, Li J X, Xue G Q, Yan G, Su D K, Xiao B, Chen L and Fan X. 2008. Discovery of sharang large-scale porphyry molybdenum deposit, the first single Mo deposit in Tibet and its significance[J]. Geology in China, 35(6): 1101-1112(in Chinese with English abstract).

Qin K Z, Su B X, Sakyi P A, Tang D M, Li X H, Sun H, Xiao Q H and Liu P P. 2011. SIMS zircon U-Pb geochronology and Sr-Nd isotopes of Ni-Cu-bearing mafic-ultramafic intrusions in eastern Tianshan and Beishan in correlation with flood basalts in Tarim basin (NW China): Constraints on a Ca. 280 Ma mantle plume[J]. American Journal of Science, 311(3): 237-260.

Qin K Z, Zhai M G, Li G M, Zhao J X, Zeng Q D, Gao J, Xiao W J, Li J L and Sun S. 2017. Links of collage orogenesis of multiblocks and crust evolution to characteristic metallogeneses in China[J]. Acta Petrologica Sinica, 33(2): 305-325(in Chinese with English abstract).

Qu P, Yang W B, Niu H C, Li N B and Wu D. 2021. Apatite fingerprints on the magmatic-hydrothermal evolution of the Daheishan giant porphyry Mo deposit, NE China[J]. Geological Society of America Bulletin, (in press).

Qu X M, Hou Z Q and Li Y G. 2004. Melt components derived from a subducted slab in late orogenic ore-bearing porphyries in the Gangdese copper belt, southern Tibetan Plateau[J]. Lithos, 74(3-4): 131-148.

Qu X M and Xin H B. 2006a. Ages and tectonic environment of the Bangong Co porphyry copper belt in western Tibet, China[J]. Geological Bulletin of China, 25(7): 792-799(in Chinese with English abstract).

Qu X M, Hou Z Q, Mo X X, Dong G C, Xu W Y and Xin H B. 2006b. Relationship between Gangdese porphyry copper deposits and uplifting of southern Tibet plateau: Evidence from multistage zircon of ore-bearing porphyries[J]. Mineral Deposits, 25(4): 388-400(in Chinese with English abstract).

Qu X M, Hou Z Q, Zaw K and Li Y G. 2007. Characteristics and genesis of Gangdese porphyry Cu deposits in the southern Tibetan Plateau: Preliminary geochemical and geochronological results[J]. Ore Geology Reviews, 31: 205-223.

Ren J S, Deng P, Xiao L W, Niu B G and Wang J. 2006. Petroliferous provinces in China and the world: A comparison from tectonic point of view[J]. Acta Geologica Sinica, 80(10): 1491-1500(in Chinese with English abstract).

Richards J P. 2003. Tectono-magmatic precursors for porphyry Cu-(Mo-Au) deposit formation[J]. Econ. Geol., 98(8): 1515-1533.

Richards J P and Kerrich R. 2007. Special paper: Adakite-like rocks: Their diverse origins and questionable role in metallogenesis[J]. Econ. Geol., 102(4): 537-576.

Richards J P. 2009. Postsubduction porphyry Cu-Au and epithermal Au deposits: Products of remelting of subduction-modified lithosphere[J]. Geology, 37(3): 247-250.

Richards J P. 2011. Magmatic to hydrothermal metal fluxes in convergent and collided margins[J]. Ore Geology Reviews, 40(1): 1-26.

Richards J P, Spell T, Rameh E, Razique A and Fletcher T. 2012. High Sr/Y magmas reflect arc maturity, high magmatic water content, and porphyry Cu±Mo±Au potential: Examples from the Tethyan arcs of central and eastern Iran and western Pakistan[J]. Econ. Geol., 107(2): 295-332.

Richards J P. 2013. Giant ore deposits formed by optimal alignments and combinations of geological processes[J]. Nature Geoscience, 6 (11): 911-916.

Richards J P. 2015a. Tectonic, magmatic, and metallogenic evolution of the Tethyan orogen: From subduction to collision[J]. Ore Geology Reviews, 70: 323-345.

Richards J P. 2015b. The oxidation state, and sulfur and Cu contents of arc magmas: Implications for metallogeny[J]. Lithos, 233: 27-45.

Richards J P and Şengör A M C. 2017. Did Paleo-Tethyan anoxia kill arc magma fertility for porphyry copper formation[J]? Geology, 45 (7): 591-594.

Ridolfi F, Puerini M, Renzulli A, Menna M and Toulkeridis T. 2008. The magmatic feeding system of El Reventador volcano (Sub-Andeanzone, Ecuador) constrained by texture, mineralogy and thermobarometry of the 2002 erupted products[J]. Journal of Volcanology and Geothermal Research, 176(1): 94-106.

Ridolfi F, Renzulli A and Puerini M. 2010. Stability and chemical equilibrium of amphibole in calc-alkaline magmas: An overview, new thermobarometric formulations and application to subduction-related volcanoes[J]. Contributions to Mineralogy and Petrology, 160(1): 45-66.

Robb L. 2005. Introduction to ore-forming processes[M]. Blackwell Publishing. 735-736.

Rui Z Y, Zhang L S, Chen Z Y, Wang L S, Liu Y L and Wang Y T. 2004. Approach on source rock or source region of porphyry copper deposits[J]. Acta Petrologica Sinica, 20(2): 229-238(in Chinese with English abstract).

Sen C and Dunn T. 1994. Dehydration melting of a basaltic composition amphibolite at 1.5 and 2.0 GPa: Implications for the origin of adakites[J]. Contributions to Mineralogy and Petrology, 117(4): 394-409.

Seton M, Müller R D, Zahirovic S, Gaina C, Torsvik T H, Shephard G, Talsma A, Gurnis M, Turner M, Maus S and Chandler M. 2012. Global continental and ocean basin reconstructions since 200 Ma[J]. Earth-Science Reviews, 113(3-4): 212-270.

Sharp W D and Clague D A. 2006. 50 Ma initiation of Hawaiian-Emperor bend records major change in Pacific plate motion[J]. Science, 313(5791): 1281-1284.

Shen Y, Zheng Y C, Hou Z Q, Zhang A P, Huizenga J M, Wang Z X and Wang L. 2021. Petrology of the Machangqing complex in southeastern Tibet: Implications for the Genesis of potassium-rich adakite-like intrusions in collisional zones[J]. Journal of Petrology, 62(11): 1-40.

Shu Q H, Chang Z S, Lai Y, Hu X L, Wu H Y, Zhang Y, Wang P, Zhai D G and Zhang C. 2019. Zircon trace elements and magma fertility: Insights from porphyry (-skarn) Mo deposits in NE China[J]. Mineralium Deposita, 54(5): 645-656.

Sillitoe R H. 1972. A plate tectonic model for the origin of porphyry copper deposits[J]. Econ. Geol., 67: 184-197.

Sillitoe R H. 1997. Characteristics and controls of the largest porphyry copper-gold and epithermal gold deposits in the circum-Pacific region[J]. Australian Journal of Earth Sciences, 44: 373-388.

Sillitoe R H. 1998. Major regional factors favoring large size, high hypogene grade, elevated gold content and supergene oxidation and enrichment of porphyry copper deposits[A]. In: Porter T M, ed. Porphyry and hydrothermal copper and gold deposits: A Global Perspective[C]. Perth, 1998, Conference Proceedings: Glenside, South Australia, Australian Mineral Foundation. 21-34.

Sillitoe R H. 2010. Porphyry copper system[J]. Econ. Geol., 105(1): 3-

41.

Sillitoe R H. 2018. Why no porphyry copper deposits in Japan and South Korea[J]? Resource Geology, 68(2): 107-125.

Sinclair W D. 2007. Porphyry deposit. Mineral deposits of Canada: A synthesis of major deposit-types, district metallogeny, the evolution of geological provinces, and exploration methods[M]. Geological Association of Canada, Mineral Deposit Division, Special Publication, 5:223-243.

Singer D A, Berger V I, Menzie W D and Berger B R. 2005. Porphyry copper deposit density[J]. Econ. Geol., 100(3): 491-514.

Singer D A, Berger V I and Moring B C. 2008. Porphyry copper deposits of the world: Database and grade and tonnage models[J]. U.S. Geological Survey Open-File Report 2008-1155, 45.

Sun B K, Ruan B X, Lü X B, Tuohan B and Ratchford M E. 2020. Geochronology and geochemistry of the igneous rocks and ore-forming age in the Huangtan AuCu deposit in the Kalatag district, eas-tern Tianshan, NW China: Implications for petrogenesis, geodynamic setting, and mineralization[J]. Lithos, 368-369: 105594.

Sun W D, Ding X, Hu Y H and Li X H. 2007. The golden transformation of the Cretaceous plate subduction in the West Pacific[J]. Earth and Planetary Science Letters, 262(3-4): 533-542.

Sun W D, Ling M X, Wang F Y, Ding X, Hu Y H, Zhou J B and Yang X Y. 2008. Pacific plate subduction and Mesozoic geological event in eastern China[J]. Bulletin of Mineralogy, Petrology and Geochemistry, 27(3): 218-225(in Chinese with English abstract).

Sun W D, Ling M X, Yang X Y, Fan W M, Ding X and Liang H Y. 2010. Ridge subduction and porphyry copper-gold mineralization: An overview[J]. Science China Earth Sciences, 53(4): 475-484.

Sun W D, Zhang H, Ling M X, Ding X, Chung S L, Zhou J B, Yang X Y and Fan W M. 2011. The genetic association of adakites and Cu-Au ore deposits[J]. International Geology Review, 53(5-6): 691-703.

Sun W D, Yang X Y, Fan W M and Wu F Y. 2012. Mesozoic large scale magmatism and mineralization in South China: Preface[J]. Lithos, 150: 1-5.

Sun W D, Liang H Y, Ling M X, Zhan M Z, Ding X, Zhang H, Yang X Y, Li Y L, Ireland T R and Wei Q R. 2013. The link between reduced porphyry copper deposits and oxidized magmas[J]. Geochimica et Cosmochimica Acta, 103(1): 263-275.

Sun W D, Huang R F, Li H, Hu Y B, Zhang C C, Sun S J, Zhang L P, Ding X, Li C Y and Zartman R E. 2015. Porphyry deposits and oxidized magmas[J]. Ore Geology Reviews, 65: 97-131.

Sun W D, Li C Y, Ling M X, Ding X, Yang X Y, Liang H Y, Zhang H and Fan W M. 2015. The geochemical behavior of molybdnum and mineralization[J]. Acta Petrologica Sinica, 31(7): 1807-1817 (in Chinese with English abstract).

Sun W D, Wang J T, Zhang L P, Zhang C C, Li H, Ling M X, Ding X, Li C Y and Liang H Y. 2017. The formation of porphyry copper deposits[J]. Acta Geochimica, 36(1): 9-15.

Sun W D, Liu L J, Hu Y B, Ding W, Liu J Q, Ling M X, Ding X, Zhang Z F, Sun X I, Li C Y, Li H and Fan W M. 2018. Post-ridge-subduction acceleration of the Indian plate induced by slab roll-back[J]. Solid Earth Sciences, 3(1): 1-7.

Sun W D, Zhang L P, Li H and Liu X. 2020. The synchronic Cenozoic subduction initiations in the West Pacific induced by the closure of the Neo-Tethys Ocean[J]. Science Bulletin, 65(24): 2068-2071.

Sun W D and Li C Y. 2020. The geochemical behavior and mineralization of critical metals[J]. Acta Petrologica Sinica, 36(1): 1-4(in Chinese with English abstract).

Sun X, Lu Y J, McCuaig T C, Zheng Y Y, Chang H F, Guo F and Xu L J. 2018. Miocene ultrapotassic, high-Mg dioritic, and adakite-like rocks from Zhunuo in southern Tibet: Implications for mantle metasomatism and porphyry copper mineralization in collision orogens[J]. Journal of Petrology, 59(3): 341-386.

Tafti R, Lang J R, Mortensen J K, Oliver J L and Rebagliati C M. 2014. Geology and geochronology of the Xietongmen (Xiongcun) Cu-Au porphyry district, southern Tibet, China[J]. Econ. Geol., 109(7): 1967-2001.

Tang M, Lee C T A, Ji W Q, Wang R and Costin G. 2020. Crustal thickening and endogenic oxidation of magmatic sulfur[J]. Science Advances, 6(31): eaba6342.

Tassara S, González-Jiménez J M, Reich M, Schilling M E, Morata D, Begg G and Barra F. 2017. Plume-subduction interaction forms large auriferous provinces[J]. Nature Communications, 8: 1-7.

Trail D, Watson E B and Tailby N D. 2012. Ce and Eu anomalies in zircon as proxies for the oxidation state of magma[J]. Geochimica et Cosmochimica Acta, 97(1): 70-87.

Turner S, Arnaud N, Liu J, Rogers N, Hawkesworth C, Harris N, Kelley S, Van Calsteren P and Deng W. 1996. Post-collision, shoshonitic volcanism on the Tibetan Plateau: Implications for convective thinning of the lithosphere and the source of ocean island basalts[J]. Journal of Petrology, 37(1): 45-71.

Wainwright A J, Tosdal R M, Wooden J L, Mazdab F K and Friedman R M. 2011. U-Pb (zircon) and geochemical constraints on the age, origin, and evolution of Paleozoic arc magmas in the Oyu Tolgoi porphyry Cu-Au district, southern Mongolia[J]. Gondwana Research, 19(3): 764-787.

Wang C, Ding L, Zhang L Y, Kapp P, Pullen A and Yue Y H. 2016. Petrogenesis of Middle-Late Triassic volcanic rocks from the Gangdese belt, southern Lhasa terrane: Implications for early subduction of Neo-Tethyan oceanic lithosphere[J]. Lithos, 262: 320-333.

Wang D Z, Hu R Z, Hollings P, Bi X W, Zhong H, Pan L C, Leng C B, Huang M L and Zhu J J. 2021. Remelting of a Neoproterozoic arc root: Origin of the Pulang and Songnuo porphyry Cu deposits, Southwest China[J]. Mineralium Deposita, 56: 1043-107.

Wang F Y, Ling M X, Ding X, Hu Y H, Zhou J B, Yang X Y, Liang H Y, Fan W M and Sun W D. 2011. Mesozoic large magmatic events and mineralization in SE China: Oblique subduction of the Pacific plate[J]. International Geology Review, 53(5-6): 704-726.

Wang Q, Zhao Z H, Xiong X L and Xu J F. 2001. Melting of the underplated basaltic lower crust: Evidence from the Shaxi adakitic sodic quartz diorite-porphyrites, Anhui Province, China[J]. Geochimic, 30(4): 353-362(in Chinese with English abstract).

Wang Q, Zhao Z H, Xu J F, Bai Z H, Wang J X and Liu C X. 2004. The geochemical comparison between the Tongshankou and Yinzu adakitic intrusive rocks in southeastern Hubei: (delaminated) Lower crustal melting and the genesis of porphyry copper deposit[J]. Acta Petrologica Sinica, 20(2): 351-360(in Chinese with English abstract).

Wang Q, Xu J F, Jian P, Bao Z W, Zhao Z H, LI C F, Xiong X L and Ma J L. 2006. Petrogenesis of adakitic porphyries in an extensional tectonic setting, Dexing, South China: Implications for the genesis of porphyry copper mineralization[J]. Journal of Petrology, 47(1): 119-144.

Wang R, Richards J P, Hou Z Q, Yang Z M, Gou Z B and Andrew D S. 2014. Increasing magmatic oxidation state from Paleocene to Miocene in the eastern Gangdese belt, Tibet: Implication for collision-related porphyry Cu-Mo±Au mineralization[J]. Econ. Geol., 109 (7): 1943-1965.

Wang R, Richards J P, Hou Z Q, An F and Creaser R A. 2015. Zircon U-Pb age and Sr-Nd-Hf-O isotope geochemistry of the Paleocene-Eocene igneous rocks in western Gangdese: Evidence for the timing of Neo-Tethyan slab breakoff[J]. Lithos, 224-225: 179-194.

Wang R, Collins W J, Weinberg R F, Li J X, Li Q Y, He W Y, Richards J P, Hou Z Q, Zhou L M and Stern R A. 2016. Xenoliths in ultrapotassic volcanic rocks in the Lhasa block: Direct evidence for crust-mantle mixing and metamorphism in the deep crust[J]. Contributions to Mineralogy and Petrology, 171(7): 1-19.

Wang R, Tafti R, Hou Z Q, Shen Z C, Guo N, Evans N, Jeon H, Li Q Y and Li W K. 2017. Across-arc geochemical variation in the Jurassic magmatic zone, southern Tibet: Implication for continental arc-related porphyry Cu-Au mineralization[J]. Chemical Geology, 451: 116-134.

Wang R, Weinberg R F, Collins W J, Richards J P and Zhu D C. 2018. Origin of postcollisional magmas and formation of porphyry Cu deposits in southern Tibet[J]. Earth-Science Reviews, 181: 122-143.

Wang R, Zhu D C, Wang Q, Hou Z Q, Yang Z M, Zhao Z D and Mo X X. 2020. Porphyry mineralization in the Tethyan orogen[J]. Science China Earth Sciences, 63(12): 2042-2067.

Wang R, Weinberg R F, Zhu D C, Hou Z Q and Yang Z M. 2022. The impact of a tear in the subducted Indian plate on the Miocene geology of the Himalayan-Tibetan orogen[J]. Geological Society of America Bulletin, 134(3-4): 681-690.

Wang Y J, Fan W M, Zhang G W and Zhang Y H. 2013. Phanerozoic tectonics of the South China Block: Key observations and controversies[J]. Gondwana Research, 23(4): 1273-1305.

Waters L E, Andrews B J and Lange R A. 2015. Rapid crystallization of plagioclase phenocrysts in silicic melts during fluid-saturated ascent: Phase equilibrium and decompression experiments[J]. Journal of Petrology, 56(5): 981-1006.

Watson E B and Harrison T M. 1983. Zircon saturation revisited: Temperature and composition effects in a variety of crustal magma types[J]. Earth and Planetary Science Letters, 64(2): 295-304.

Wei S G, Tang J X, Song Y, Liu Z B, Feng J and Li Y B. 2017. Early Cretaceous bimodal volcanism in the Duolong Cu mining district, western Tibet: Record of slab breakoff that triggered Ca. 108-113 Ma magmatism in the western Qiangtang terrane[J]. Journal of Asian Earth Sciences, 138: 588-607.

Wilkinson J J. 2013. Triggers for the formation of porphyry ore deposits in magmatic arcs[J]. Nature Geoscience, 6: 917-925.

Williams H M, Turner S P, Pearce J A, Kelley S P and Harris N. 2004. Nature of the source regions for post-collisional, potassic magmatism in southern and northern Tibet from geochemical variations and inverse trace element modelling[J]. Journal of Petrology, 45 (3): 555-607.

Williamson B J, Herrington R J and Morris A. 2016. Porphyry copper enrichment linked to excess aluminium in plagioclase[J]. Nature Geoscience, 9(3): 237-241.

Windley B F, Alexeiev D, Xiao W J, Kröner A and Badarch G. 2007. Tectonic models for accretion of the Central Asian Orogenic Belt[J]. Journal of the Geological Society, 164(1): 31-47.

Wu F Y, Wan B, Zhao L, Xiao W J and Zhu R X. 2020. Tethyan geodynamics[J]. Acta Petrologica Sinica, 36(6): 1627-1674(in Chinese with English abstract).

Xia X P, Cui Z X, Li W C, Zhang W F, Yang Q, Hui H J and Lai C K. 2019. Zircon water content: Reference material development and simultaneous measurement of oxygen isotopes by SIMS[J]. Journal of Analytical Atomic Spectrometry, 34(6): 1088-1097.

Xiao B, Chen H Y, Hollings P, Han J S, Wang Y F, Yang J T and Cai K. 2017. Magmatic evolution of the Tuwu-Yandong porphyry Cu belt, NW China: Constraints from geochronology, geochemistry and Sr-Nd-Hf isotopes[J]. Gondwana Research, 43: 74-91.

Xiao W J, Huang B C, Han C M, Sun S and Li J L. 2010. A review of the western part of the Altaids: A key to understanding the architecture of accretionary orogens[J]. Gondwana Research, 18(2-3): 253-273.

Xu B, Hou Z Q, Griffin W L, Lu Y J, Belousova E, Xu J F and O'Reilly S Y. 2021. Recycled volatiles determine fertility of porphyry deposits in collisional settings[J]. American Mineralogist, 106(4): 656-661.

Xu J F, Shinjo R, Defant M J, Wang Q and Rapp R P. 2002. Origin of Mesozoic adakitic intrusive rocks in the Ningzhen area of East China: Partial melting of delaminated lower continental crust[J]? Geology, 30(12): 1111-1114.

Xu W, Zhu D C, Wang Q, Weinberg R F, Wang R, Li S M, Zhang L L and Zhao Z D. 2019. Constructing the early mesozoic Gangdese crust in southern Tibet by hornblende dominated magmatic differentiation[J]. Journal of Petrology, 60(3): 515-552.

Xue C J, Zhao X B and Mo X X. 2016. Problem on porphyry Cu-Au metallogenic environment in Central Asian: An overview[J]. Acta Petrologica Sinica, 32(5): 1249-1261(in Chinese with English abstract).

Yang L Q, Gao X and He W Y. 2015. Late Cretaceous porphyry metallogenic system of the Yidun arc, SW China[J]. Acta Petrologica Sinica, 31(11): 3155-3170(in Chinese with English abstract).

Yang L Q, Deng J, Dilek Y, Meng J Y, Gao X, Santosh M, Wang D and Yan H. 2016. Melt source and evolution of I-type granitoids in the SE Tibetan Plateau: Late Cretaceous magmatism and mineralization driven by collision-induced transtensional tectonics[J]. Lithos, 245: 258-273.

Yang L Q, Deng J, Gao X, He W Y, Meng J Y, Santosh M, Yu H J, Yang Z and Wang D. 2017. Timing of formation and origin of the Tongchanggou porphyry-skarn deposit: Implications for Late Cretaceous Mo-Cu metallogenesis in the southern Yidun Terrane, SE Tibetan Plateau[J]. Ore Geology Reviews, 81: 1015-1032.

Yang Z M, Hou Z Q, Yang Z S, Wang S X, Wang G R, Tian S H, Wen D Y, Wang Z L and Liu Y C. 2008. Genesis of porphyries and tectonic controls on the Narigongma porphyry Mo(- Cu) deposit, southern Qinghai[J]. Acta Petrologica Sinica, 24(3): 489-502(in Chinese with English abstract).

Yang Z M, Hou Z Q, White N C, Chang Z S, Li Z Q and Song Y C. 2009. Geology of the post-collisional porphyry copper-molybdenum deposit at Qulong, Tibet[J]. Ore Geology Reviews, 36: 133-159.

Yang Z M and Hou Z Q. 2009. Porphyry Cu deposits in collisional orogen setting: A preliminary genetic model[J]. Mineral Deposits, 28 (5): 515-538(in Chinese with English abstract).

Yang Z M, Hou Z Q, Xu J F, Bian X F, Wang G R, Yang Z S, Tian S H, Liu Y C and Wang Z L. 2014. Geology and origin of the post-collisional Narigongma porphyry Cu-Mo deposit, southern Qinghai, Tibet[J]. Gondwana Research, 26(2): 536-556.

Yang Z M, Lu Y J, Hou Z Q and Chang Z S. 2015. High-Mg diorite from Qulong in southern Tibet: Implications for the genesis of adakite-like intrusions and associated porphyry Cu deposits in collisional orogens[J]. Journal of Petrology, 56(2): 227-254.

Yang Z M, Goldfarb R and Chang Z S. 2016. Generation of postcollisional porphyry copper deposits in southern Tibet triggered by subduction of the Indian continental plate[M]. Society of Economic Geologists, Special Publication. 19: 279-300.

Yang Z M and Cooke D R. 2019. Porphyry Cu deposits in China[M]. Society of Economic Geologists, Special Publication. 22: 133-187.

Yang Z M, Hou Z Q, Zhou L M and Zhou Y W. 2020. Critical elements in porphyry copper deposits of China[J]. Chinese Science Bulletin, 65(33): 3653-3664(in Chinese with English abstract).

Yuan C, Sun M, Wilde S, Xiao W J, Xu Y G, Long X P and Zhao G C. 2010. Post-collisional plutons in the Balikun area, East Chinese Tianshan: Evolving magmatism in response to extension and slab break-off[J]. Lithos, 119(3-4): 269-288.

Yuan H L, Liu X M, Liu Y S, Gao S and Ling W L. 2006. Geochemistry and U-Pb zircon geochronology of Late-Mesozoic lavas from Xishan, Beijing[J]. Science in China (Series D: Earth Sciences), 49(1): 50-67.

Zajacz Z and Halter W. 2009. Copper transport by high temperature, sulfur-rich magmatic vapor: Evidence from silicate melt and vapor inclusions in a basaltic andesite from the Villarrica volcano (Chile)[J]. Earth and Planetary Science Letters, 282(1-4): 115-121.

Zajacz Z, Seo J H, Candela P A, Piccoli P M, Heinrich C A and Guillong M. 2010. Alkali metals control the release of gold from volatile-rich magmas[J]. Earth and Planetary Science Letters, 297(1-2): 50-56.

Zhang C C, Sun W D, Wang J T, Zhang L P, Sun S J and Wu K. 2017. Oxygen fugacity and porphyry mineralization: A zircon perspective of Dexing porphyry Cu deposit, China[J]. Geochimica et Cosmochimica Acta, 206(1): 343-363.

Zhang D H and Audétat A. 2017. What caused the formation of the giant Bingham Canyon porphyry Cu-Mo-Au deposit? Insights from melt inclusions and magmatic sulfides[J]. Econ. Geol., 112(2): 221-244.

Zhang H L, Hirschmann M M, Cottrell E, Newville M and Lanzirotti A. 2016. Structural environment of iron and accurate determination of $Fe^{3+}/\sum Fe$ ratios in andesitic glasses by XANES and Mössbauer spectroscopy[J]. Chemical Geology, 428: 48-58.

Zhang H R, Hou Z Q and Yang Z M. 2010. Metallogenesis and geodynamics of Tethyan metallogenic domain: A review[J]. Mineral Deposits, 29(1): 113-133(in Chinese with English abstract).

Zhang H R, Yang Z M and Song Y C. 2013. The study progress of Sar Cheshmeh Cu-Mo-Au deposit, Iran[J]. Geological Science and Technology Information, 32(5): 167-173(in Chinese with English abstract).

Zhang H T, Chen R Y and Han F L. 2004. Reunderstanding of metallogenic geological conditions of porphyry copper deposits in China[J]. Mineral Deposits, 23(2): 150-163(in Chinese with English abstract).

Zhang Q, Wang Y L and Wang Y. 2001. Preliminary study on the components of the lower crust in East China Plateau during Yanshanian Period: Constraints on Sr and Nd isotopic compositions of adakite-like rocks[J]. Acta Petrologica Sinica, 17(4): 505-513(in Chinese with English abstract).

Zhang Q, Wang Y, Liu W and Wang Y L. 2002. Adakite: Its characteristics and implications[J]. Geological Bulletin of China, 21(7): 431-435(in Chinese with English abstract).

Zhang Z M, Dong X, Xiang H, He Z Y and Liou J G. 2014. Metagabbros of the Gangdese arc root, South Tibet: Implications for the growth of continental crust[J]. Geochimica et Cosmochimica Acta, 143: 268-284.

Zhao C, Qin K Z, Song G X, Li G M, Li Z Z, Pang X Y and Wang L. 2018. Petrogenesis and tectonic setting of ore-related porphyry in the Duobaoshan Cu deposit within the eastern Central Asian Orogenic Belt, Heilongjiang Province, NE China[J]. Journal of Asian Earth Sciences, 165: 352-370.

Zhao J X, Qin K Z and Li G M. 2014. Collision-related genesis of the Sharang porphyry molybdenum deposit, Tibet: Evidence from zircon U-Pb ages, Re-Os ages and Lu-Hf isotopes[J]. Ore Geology Reviews, 56: 312-326.

Zhao J X, Qin K Z, Li G M, Cao M J, Evans N J, McInnes B I A, Li J

X, Xiao B and Chen L. 2015. The exhumation history of collision-related mineralizing systems in Tibet: Insights from thermal studies of the Sharang and Yaguila deposits, Central Lhasa[J]. Ore Geology Reviews, 65: 1043-1061.

Zhao J X, Su B X, Uysal İ, Aydin F, Xiao Y, Sen C, Hui K X and Qin K Z. 2021. Evolution of magma oxidation states and volatile components in the Cenozoic porphyry ore systems in the western Turkey, Tethyan domain: Constraints from the compositions of zircon and apatite[J]. Acta Petrologica Sinica, 37(8): 2339-2363(in Chinese with English abstract).

Zhao X B, Xue C J, Chi G X, Mo X X, Nurtaev B and Zhang G Z. 2017. Zircon and molybdenite geochronology and geochemistry of the Kalmakyr porphyry Cu-Au deposit, Almalyk district, Uzbekistan: Implications for mineralization processes[J]. Ore Geology Reviews, 86: 807-824.

Zheng Y C, Liu S A, Wu C D, Griffin W L, Li Z Q, Xu B, Yang Z M, Hou Z Q and O'Reilly S Y. 2019. Cu isotopes reveal initial Cu enrichment in sources of giant porphyry deposits in a collisional setting[J]. Geology, 47(2): 135-138.

Zheng Y C, Wu C D, Tian S L, Hou Z Q, Fu Q and Zhu D C. 2020. Magmatic and structural controls on the tonnage and metal associations of collision-related porphyry copper deposits in southern Tibet[J]. Ore Geology Reviews, 122: 103509.

Zheng Y C, Shen Y, Wang L, Griffin W L and Hou Z Q. 2021. Collision-related porphyry Cu deposits formed by input of ultrapotassic melts into the sulfide-rich lower crust[J]. Terra Nova, 33(6): 582-589.

Zheng Y F, Chen R X, Xu Z and Zhang S B. 2016. The transport of water in subduction zones[J]. Science China Earth Sciences, 59(4): 651-682.

Zheng Y F, Mao J W, Chen Y J, Sun W D, Ni P and Yang X Y. 2019. Hydrothermal ore deposits in collisional orogens[J]. Science Bulletin, 64(3): 205-212.

Zhou Q, Jiang Y H, Zhao P, Liao S Y and Jin G D. 2012. Origin of the Dexing Cu-bearing porphyries, SE China: Elemental and Sr-Nd-Pb-Hf isotopic constraints[J]. International Geology Review, 54 (5): 572-592.

Zhou T C, Zeng Q D, Chu S X, Zhou L L and Yang Y H. 2018. Magmatic oxygen fugacities of porphyry Mo deposits in the East Xing'an-Mongolian Orogenic Belt (NE China) with metallogenic implications[J]. Journal of Asian Earth Sciences, 165: 145-159.

Zhou X M and Li W X. 2000. Origin of Late Mesozoic igneous rocks in southeastern China: Implications for lithosphere subduction and underplating of mafic magmas[J]. Tectonophysics, 326(3-4): 269-287.

Zhou X M, Sun T, Shen W Z, Shu L S and Niu Y L. 2006. Petrogenesis of Mesozoic granitoids and volcanic rocks in South China: A response to tectonic evolution[J]. Episodes, 29(1): 26-33.

Zhou Y, Xu B, Hou Z Q, Wang R, Zheng Y C and He W Y. 2019. Petrogenesis of Cenozoic high-Sr/Y shoshonites and associated mafic microgranular enclaves in an intracontinental setting: Implications for porphyry Cu-Au mineralization in western Yunnan, China[J]. Lithos, 324-325: 39-54.

Zhu D C, Wang Q, Zhao Z D, Chung S L, Cawood P A, Niu Y, Liu S A, Wu F Y and Mo X X. 2015. Magmatic record of India-Asia collision[J]. Scientific Reports, 5: 1-9.

Zhu D C, Wang Q, Cawood P A, Zhao Z D and Mo X X. 2017. Raising the Gangdese Mountains in southern Tibet[J]. Journal of Geophysical Research: Solid Earth, 122: 214-223.

Zhu D C, Wang Q, Chung S L, Cawood P A and Zhao Z D. 2019. Gangdese magmatism in southern Tibet and India-Asia convergence since 120 Ma[J]. Geological Society, London, Special Publications, 483(1): 583-604.

Zhu R X and Xu Y G. 2019. The subduction of the West Pacific plate and the destruction of the North China Craton[J]. Science China Earth Sciences, 62(9): 1340-1350.

Zhu R X, Zhao P and Zhao L. 2022. Tectonic evolution and geodynamics of the Neo-Tethys Ocean[J]. Science China Earth Sciences, 65(1):1-24.

附中文参考文献

毕献武, 胡瑞忠, 彭建堂, 吴开兴, 苏文超, 战新志. 2005. 姚安和马厂箐富碱侵入岩体的地球化学特征[J]. 岩石学报, 21(1): 113-124.

陈衍景, 翟明国, 蒋少涌. 2009. 华北大陆边缘造山过程与成矿研究的重要进展和问题[J]. 岩石学报, 25(11): 2695-2726.

邓军, 侯增谦, 莫宣学, 杨立强, 王庆飞, 王长明. 2010. 三江特提斯复合造山与成矿作用[J]. 矿床地质, 29(1): 37-42.

范羽, 周涛发, 张达玉, 袁峰, 范裕, 任志, White N C. 2014. 中国钼矿床的时空分布及成矿背景分析[J]. 地质学报, 88(4): 784-804.

高俊, 朱明田, 王信水, 洪涛, 李光明, 李继磊, 肖文交, 秦克章, 曾庆栋, 申萍, 徐兴旺, 张招崇, 周建波,赖勇, 张晓晖, 孙景贵, 万博, 王博. 2019. 中亚成矿域斑岩大规模成矿特征:大地构造背景、流体作用与成矿深部动力学机制[J]. 地质学报, 93(1): 24-71.

耿全如, 潘桂棠, 王立全, 彭智敏, 张璋. 2011. 班公湖-怒江带、羌塘地块特提斯演化与成矿地质背景[J]. 地质通报, 30(8): 1261-1274.

侯增谦, 高永丰, 孟祥金, 曲晓明, 黄卫. 2004a. 西藏冈底斯中新世斑岩铜矿带: 埃达克质斑岩成因与构造控制[J]. 岩石学报, 20(2): 239-248.

侯增谦, 杨岳清, 曲晓明, 黄典豪, 吕庆田, 王海平, 余金杰, 唐绍华. 2004b. 三江地区义敦岛弧造山带演化和成矿系统[J]. 地质学报, 78(1): 109-120.

侯增谦, 莫宣学, 杨志明, 王安建, 潘桂棠, 曲晓明, 聂凤军. 2006a. 青藏高原碰撞造山带成矿作用: 构造背景、时空分布和主要类型[J]. 中国地质, 33(2): 340-351.

侯增谦, 杨竹森, 徐文艺, 莫宣学, 丁林, 高永丰, 董方浏, 李光明, 曲晓明, 李光明, 赵志丹, 江思宏, 孟祥金, 李振清, 秦克章, 杨志明. 2006b. 青藏高原碰撞造山带:I. 主碰撞造山成矿作用[J]. 矿床地质, 25(4): 337-358.

侯增谦, 潘小菲, 杨志明, 曲晓明. 2007. 初论大陆环境斑岩铜矿[J].

现代地质, 21(2): 332-351.
侯增谦, 杨志明. 2009. 中国大陆环境斑岩型矿床:基本地质特征、岩浆热液系统和成矿概念模型[J]. 地质学报, 83(12): 1779-1817.
侯增谦, 王涛. 2018. 同位素填图与深部物质探测(II): 揭示地壳三维架构与区域成矿规律[J]. 地学前缘, 25(6): 20-41.
侯增谦, 杨志明, 王瑞, 郑远川. 2020a. 再论中国大陆斑岩 Cu-Mo-Au 矿床成矿作用[J]. 地学前缘, 27(2): 20-44.
侯增谦, 郑远川, 卢占武, 许博, 王长明, 张洪瑞. 2020b. 青藏高原巨厚地壳: 生长、加厚与演化[J]. 地质学报, 94(10): 2797-2815.
胡瑞忠, 毛景文, 华仁民, 范蔚茗. 2015. 华南陆块陆内成矿作用[M]. 北京: 科学出版社. 1-903.
黄凡, 王登红, 王成辉, 陈郑辉, 袁忠信, 刘新星. 2014. 中国钼矿资源特征及其成矿规律概要[J]. 地质学报, 88(12): 2296-2314.
冷成彪, 陈喜连, 张静静, 马晓花, 田丰, 郭剑衡, 张乐骏. 2020. 斑岩型 Cu±Mo±Au 矿床的勘查标志: 岩石化学和矿物化学指标[J]. 地质学报, 94(11): 3189-3212.
李文昌, 伊光侯, 卢映祥, 王彦斌, 余海军, 曹晓明, 张世权. 2010. 西南“三江”格咱火山-岩浆弧中红山-属都蛇绿混杂岩带的厘定及其意义[J]. 岩石学报, 26(6): 1662-1664.
李文昌, 薛迎喜, 卢映祥, 薛顺荣, 任治机. 2014. 中国斑岩铜矿成矿规律与找矿方向[M]. 北京: 地质出版社. 1-411.
李晓峰, 华仁民, 马东升, 徐净, 张龙, 齐有强, 武丽艳, 朱艺婷. 2019. 大陆岩石圈伸展与斑岩铜矿成矿作用[J]. 岩石学报, 35(1): 76-88.
梁华英, 莫济海, 孙卫东, 张玉泉, 曾提, 胡光黔, Charllote M A. 2009. 玉龙铜矿带马拉松多斑岩体岩石学及成岩成矿系统年代学分析[J]. 岩石学报, 25(2): 385-392.
毛景文, 罗茂澄, 谢桂青, 刘军, 吴胜华. 2014. 斑岩铜矿床的基本特征和研究勘查新进展[J]. 地质学报, 88(12): 2153-2175.
莫宣学, 赵志丹, 邓晋福, 董国臣, 周肃, 郭铁鹰, 张双全, 王亮亮. 2003. 印度-亚洲大陆主碰撞过程的火山作用响应[J]. 地学前缘, 10(3): 135-148.
秦克章, 李光明, 赵俊兴, 李金祥, 薛国强, 严刚, 粟登奎, 肖波, 陈雷, 范新. 2008. 西藏首例独立钼矿——冈底斯沙让大型斑岩钼矿的发现及其意义[J]. 中国地质, 35(6): 1101-1112.
秦克章, 翟明国, 李光明, 赵俊兴, 曾庆栋, 高俊, 肖文交, 李继亮, 孙枢. 2017. 中国陆壳演化、多块体拼合造山与特色成矿的关系[J]. 岩石学报, 33(2): 305-325.
曲晓明, 辛洪波. 2006a. 藏西班公湖斑岩铜矿带的形成时代与成矿构造环境[J]. 地质通报, 25(7): 792-799.
曲晓明, 侯增谦, 莫宣学, 董国臣, 徐文艺, 辛洪波. 2006b. 冈底斯斑岩铜矿与南部青藏高原隆升之关系——来自含矿斑岩中多阶段锆石的证据[J]. 矿床地质, 25(4): 388-400.
任纪舜, 邓平, 肖藜薇, 牛宝贵, 王军. 2006. 中国与世界主要含油气区大地构造比较分析[J]. 地质学报, 80(10):1491-1500.
芮宗瑶, 张立生, 陈振宇, 王龙生, 刘玉琳, 王义天. 2004. 斑岩铜矿的源岩或源区探讨[J]. 岩石学报, 20(2): 229-238.
孙卫东, 凌明星, 汪方跃, 丁兴, 胡艳华, 周继彬, 杨晓勇. 2008. 太平洋板块俯冲与中国东部中生代地质事件[J]. 矿物岩石地球化学通报, 27(3): 218-225.
孙卫东, 李聪颖, 凌明星, 丁兴, 杨晓勇, 梁华英, 张红, 范蔚茗. 2015. 钼的地球化学性质与成矿[J]. 岩石学报, 31(7): 1807-1817.
孙卫东, 李聪颖. 2020. 元素的地球化学性质与关键金属成矿: 前言[J]. 岩石学报, 36(1): 1-4.
王强, 赵振华, 熊小林, 许继锋. 2001. 底侵玄武质下地壳的熔融:来自安徽沙溪 adakite 质富钠石英闪长玢岩的证据[J]. 地球化学, 30(4): 353-362.
王强, 赵振华, 许继峰, 白正华, 王建新, 刘成新. 2004. 鄂东南铜山口、殷祖埃达克质(adakitic)侵入岩的地球化学特征对比:(拆沉)下地壳熔融与斑岩铜矿的成因[J]. 岩石学报, 20(2): 351-360.
吴福元, 万博, 赵亮, 肖文交, 朱日祥. 2020. 特提斯地球动力学[J]. 岩石学报, 36(6): 1627-1674.
薛春纪, 赵晓波, 莫宣学. 2016. 中亚成矿域斑岩铜金成矿的地质环境问题[J]. 岩石学报, 32(5): 1249-1261.
杨立强, 高雪, 和文言. 2015. 义敦岛弧晚白垩世斑岩成矿系统[J]. 岩石学报, 31(11): 3155-3170.
杨志明, 侯增谦, 杨竹森, 王淑贤, 王贵仁, 田世洪, 温德银, 王召林, 刘英超. 2008. 青海纳日贡玛斑岩钼(铜)矿床: 岩石成因及构造控制[J]. 岩石学报, 24(3): 489-502.
杨志明, 侯增谦. 2009. 初论碰撞造山环境斑岩铜矿成矿模型[J]. 矿床地质, 28(5): 515-538.
杨志明, 侯增谦, 周利敏, 周怿惟. 2020. 中国斑岩铜矿床中的主要关键矿产[J]. 科学通报, 65(33): 3653-3664.
张洪瑞, 侯增谦, 杨志明. 2010. 特提斯成矿域主要金属矿床类型与成矿过程[J]. 矿床地质, 29(1): 113-133.
张洪瑞, 杨志明, 宋玉财. 2013. 伊朗萨尔切什梅铜-钼-金矿床研究新进展[J]. 地质科技情报, 32(5): 167-173.
张洪涛, 陈仁义, 韩芳林. 2004. 重新认识中国斑岩铜矿的成矿地质条件[J]. 矿床地质, 23(2): 150-163.
张旗, 王元龙, 王焰. 2001. 燕山期中国东部高原下地壳组成初探:埃达克质岩 Sr、Nd 同位素制约[J]. 岩石学报, 17(4): 505-513.
张旗, 王焰, 刘伟, 王元龙. 2002. 埃达克岩的特征及其意义[J]. 地质通报, 21(7): 431-435.
赵俊兴, 苏本勋, Uysal İ, Aydin F, 肖燕, Sen C, 回凯旋, 秦克章. 2021. 土耳其西部新生代斑岩成矿岩浆氧逸度-挥发份元素组成演化特征——来自锆石和磷灰石组成约束[J]. 岩石学报, 37(8): 2339-2363.